46TH TURBOMACHINERY & 33RD PUMP SYMPOSIA
HOUSTON, TEXAS | DECEMBER 11-14, 2017
GEORGE R. BROWN CONVENTION CENTER

ELECTRIC-MOTOR-DRIVEN GAS COMPRESSOR PACKAGES: STARTING METHODS FOR LARGE ELECTRICAL MOTORS AND TORSIONAL INTEGRITY

Michael Glasbrenner
Head of Control & Electrical Engineering
Voith Turbo GmbH & Co. KG
Crailsheim, Germany

Balaji Venkataraman
Manager, Rotordynamics
Solar Turbines Incorporated
San Diego, California, USA

Rainer Kurz
Manager, Systems Analysis and Field Test
Solar Turbines Incorporated
San Diego, California, USA

Ge' Juan Cole
Senior Project Developer
Williams Gas Pipeline
Houston, Texas, USA

Chester Lee
Consultant
Solar Turbines Incorporated
San Diego, California, USA

Michael Glasbrenner studied mechanical engineering and received the degree as graduate engineer (Dipl.-Ing.) from the University of Stuttgart, Germany in 2005. Since 2005, he has been working for the Voith AG. In 2008, he became head of mechatronic engineering for hydrodynamic superimposed gearboxes of Voith Turbo Wind GmbH & Co. KG. In 2014, Michael Glasbrenner took over the responsibility for Control & Electrical Engineering, Variable Speed Drives, of Voith Turbo GmbH & Co. KG.

Balaji Venkataraman is the Manager of Rotordynamics, Gas Compressor Products at Solar Turbines. He has been with Solar for over 18 years. His group is responsible for rotordynamic designs, compressor testing and fleet product quality from vibration standpoint. Balaji has extensive experience in the areas of vibrations diagnosis and resolution, seal design and damper bearings. Prior to joining Solar, Balaji had worked with Atlas Copco and had been a visiting researcher at NASA's Marshall Space Flight Center, Huntsville, AL. Balaji holds a Master's degree from Texas A&M University.

Dr. Rainer Kurz is the Manager, Systems Analysis, at Solar Turbines Incorporated in San Diego, California. His organization is responsible for analyzing compression requirements, pre-dicting compressor and gas turbine performance, for conducting application studies, and for field performance testing. Dr. Kurz attended the Universitaet der Bundeswehr in Hamburg, Germany, where he received the degree of a Dr.-Ing. in 1991. He has authored numerous publications about turbomachinery related topics, is an ASME fellow, and a member of the Turbomachinery Symposium Advisory Committee.

Ge'Juan Cole, P.E., is a Senior Project Developer at Williams Gas Pipeline. With over 14 years of experience in the oil and gas industry, he has held various positions in operations, project engineering, project management, and planning primarily focused on installing compression facilities on the Transco natural gas pipeline system. In his current role, he is responsible for leading multifunctional teams in the development of market expansion opportunities to build critical large scale pipeline transmission infrastructure necessary to meet the growing global demand for natural gas. Ge'Juan earned a BS in Mechanical Engineering from Georgia Tech, a BS in Mathematics from Morehouse College, and an M.B.A in Global Leadership from the University of Houston. He also holds a certificate in Project Management and is licensed by the Texas Board of Professional Engineers.

ABSTRACT

Electric Motor Drives in the power range from 1,000 to 60,000 HP are often used for turbomachinery applications. The electric drive systems used include electric motors with variable frequency drives (VFD), electric motors with variable speed planetary gear hydraulic drives (VSHD), and constant speed electric motors.

Two issues tend to require discussion, and a significant level of expertise to avoid problems:

First, the startup has to be accomplished without exceeding the maximum permissible voltage dip limits at the point of common coupling (PCC). In case of strong supply networks, a direct online start-up usually works. However, safe start-up solutions are also available for weak supply networks by using common starting devices. Torsional transients during the starting process have to be considered.

Therefore, this tutorial presents a rough overview of proven start-up methods for direct online operating electric motor drives. Pros and cons are discussed. Based on a starting by means of a pony-motor, which is connected to a hydrodynamic variable speed planetary gear, the run-up process is discussed in detail. It can be seen that the grid disturbances are negligible especially for synchronous main motors.

Second, the choice of drive impacts the train's torsional characteristics, shaft endurance limits and operational flexibility. Torsional integrity of the electric motor driven trains are critical to safe and reliable operation, and must be considered during the design, selection and packaging of the train's key components (motor, gearbox, couplings and the compressors).

This tutorial outlines a methodology used to ensure torsional integrity in standardized Electric-motor-driven gas compressor packages. In addition to steady-state torsional analysis, the drive harmonics from electrical sources (steady-state pulsation) and the drive's characteristics at fault-events such as phase-to-phase faults (transients) are incorporated into the torsional model to perform a complete torsional analysis. Shaft stresses are evaluated over a wide range of motor frame sizes, and consequently couplings and gearboxes. Couplings and gearboxes are designed to handle the mean torque and peak transient torques as appropriate. Torsional Acceptance criteria is set by incorporating today's best practices on the subject, API 684 guidelines [8] and GMRC guidelines [9], in addition to the OEM's historical experience. Results are presented for 45 Hz corner frequency motor drives.

INTRODUCTION

Electric-motor drives are increasingly used by the Oil & Gas industry for compression needs, involving higher power densities and speeds. The motors may be driven by Variable Frequency Drives (VFD), Variable Speed Hydraulic Drives (VSHD) or Fixed speed motors (Figure 1). Each type of drive poses unique set of advantages and challenges, both from application and technical perspectives. Technically, the choice of drive impacts the train's torsional characteristics, shaft endurance limits and operational flexibility. Torsional integrity of the EM-driven trains are critical to safe and reliable operation, and must be considered during the design, selection and packaging of the train's key components (motor, gearbox, couplings and the compressors).

The package configurations in question either use:

- A constant electric speed motor, driving the compressor via a fixed ratio gearbox
- An electric motor, where the electric power is supplied through a variable frequency drive. The motor drives the compressor either directly or via a fixed ratio gearbox. Depending on the design of the motor-VFD combination, different speed-power combinations are available (Figure 2).
- A constant speed electric motor, driving the compressor via a variable speed hydraulic drive. A variable speed hydraulic drive consists of planetary gearbox, where a hydraulic torque converter is used to vary the output speed of the gearbox for a constant input speed (Figure 3 shows the speed torque characteristic).

Figure 1: Electric Motor Driven Gas Compressors. Left: Variable frequency Drive (E-House not shown),or Constant speed Motor drive. Right : Variable Speed Hydraulic Drive.
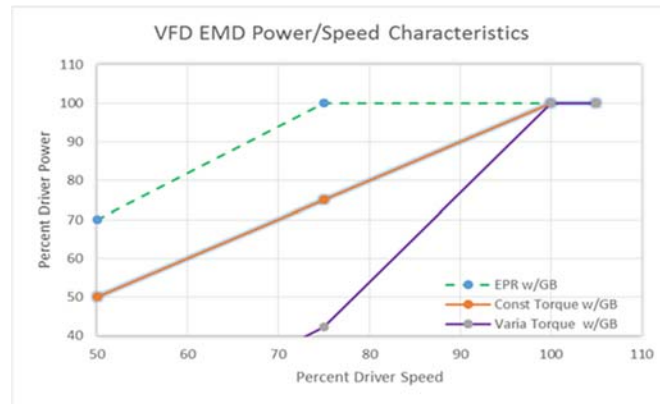

Figure 2: Speed-Torque Characteristics for different VFD configurations
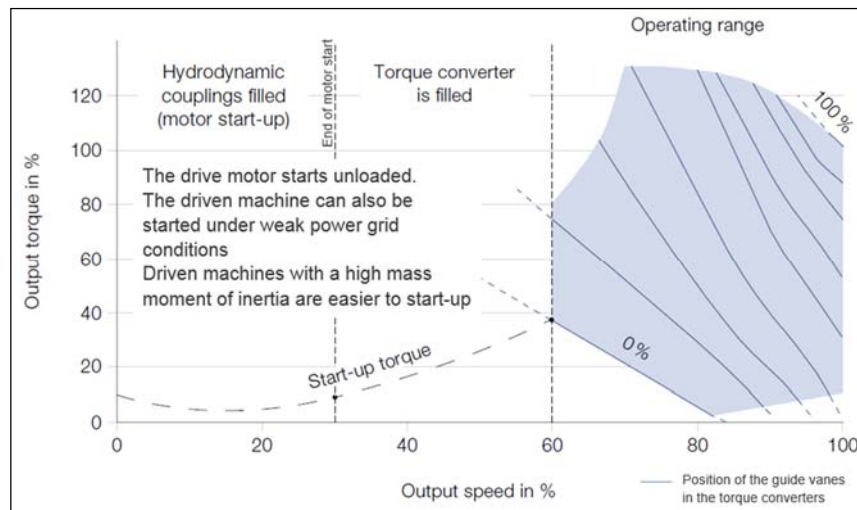

Figure 3: Speed – Torque characteristic of a typical VSHD drive.

The VFD- and VSHD options allow to control the operation of the centrifugal compressor by varying the speed, which is not only a very effective, but also a very efficient method to control the compressor operation. For a constant speed drive, the compressor operation is usually controlled via recycling gas, suction throttling or variable geometry (Kurz et al[1]), which are quite effective, but not very efficient methods. Therefore, applications where a wide variation in operating conditions is expected, and high efficiency is important, usually use compressors with drives that allow to vary the compressor speed.

STARTING BEHAVIOR OF ELECTRIC MOTORS

In all industrial sectors, asynchronous and synchronous motors are indispensable for the functional compliance with technical processes. Above all, squirrel cage motors are characterized by a high robustness, compact design and low production costs. They are scalable multiply and available for various frequencies and voltage levels.

When starting these motors, due to subtransient and transient reactions in the motor, distinct higher starting currents are induced than during normal operation. For standard motors, these are at about 5 ... 7 times the rated current. The increased current consumption mainly does not come from the acceleration or overcoming of mass moments of inertia but results from the based impedances and resistances of the electrical machine, therefore resulting in a higher reactive power demand and in a low power factor. Interacting with the connecting situations of the grid which is presented by the short-circuit capability leads to the voltage dip.

Voltage dips influence undesirably other consumers and result in a destabilization as well as disturbances of the power grid. Therefore, it is necessary to reduce them to a permissible limit. The national Grid Codes define the maximum voltage dip. In most cases, these are at max. 20 % for short and at 10 % for longer time periods at PCC.

For applications with high power requirements and in case of weak power grids, it is partly therefore necessary to take measures to limit the voltage dip. Weak grids exist especially if the main grid is far away or in case of island grids.

With a suitable design of the electric machine or by adding auxiliary systems between motor and electrical grid, the starting current, and thus the voltage dip, can be reduced effectively. This paper gives an objective insight to the following most common and approved motor starting systems:

- Low in-rush current motor
- Rotor resistance starting
- Soft starter
- Autotransformer
- Pony motor starting

The well-known variable-frequency drives (VFD) which is normally not only used as a motor starting system but rather for variable speed operation is not considered in detail. However it can be pointed out, that VFDs cause negligible voltage dips on grid side during motor start because the inverter side has its own capability to provide the required reactive power for motor. Therefore only the active power is consumed from the grid. Furthermore the motor can mobilize already at low speed a high torque. But VFDs can generally induce disturbances on the power grid as well as on the mechanical drive side like total harmonic distortions or subsynchronous vibrations.

The impact of starting has been studied by means of time-domain simulation. For this the software DIgSILENT PowerFactory [2] has been used. The models were developed in sufficient detail to study the impact that the starting process has on the supply voltage. The "RMS-type" of simulation has been performed, meaning that models that are normally used for power system stability have been selected. These models are typically also used for motor starting studies and are suitable for the calculation of quasi-stationary voltage dips. They exclude very fast electromagnetic transients, which would be relevant for studies such as insulation coordination or subsynchronous resonance [3].

For the first four starting methods, a short-circuit level of 15kA was assumed for the 132kV supply (Figure 4). The short-circuit level in the industrial power system is determined mainly by the impedance of the 132/11 kV transformer. Two 60 MVA transformers are used for future extension and to have n-1 redundancy. The total load is some 51 MVA due to consideration of additional consumers.
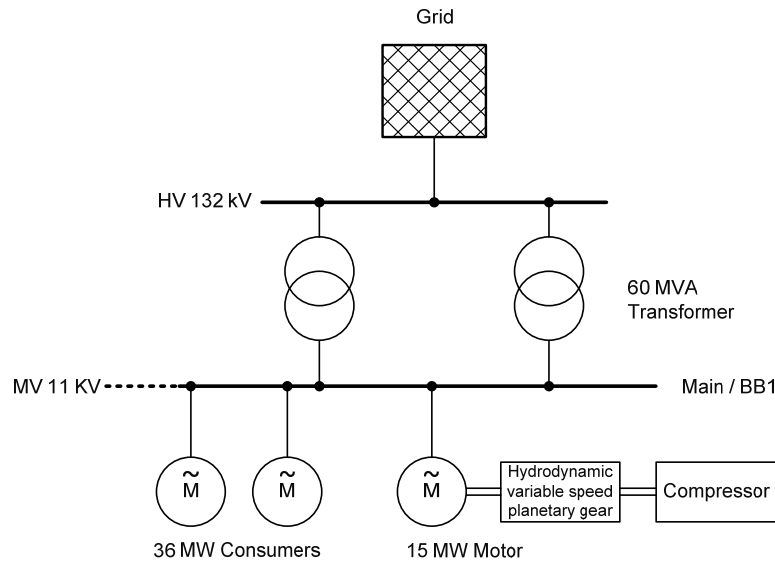
Figure 4: Power Supply - Single line diagram for 15MW asynchronous motor

To work out the advantages of the pony motor starting, a weak grid configuration with a short circuit level of 10kA was considered (Figure 15).

For this investigation, a hydrodynamic variable speed planetary gear [4] has been used as connecting member between the 15 MW motor and the compressor in order to get a drive train with variable speed and to enable a disengaged motor run-up.

In case of soft starter and autotransformer, regular squirrel cage motors can be used. Usually a pony motor is used for starting a synchronous main motor. For rotor resistance starting, a wound rotor motor type is required.

Besides the level of the voltage dip, also the duration of the voltage dip during the run-up time is of significance. The temporal magnitude is defined decisively by the counter-torque and by the mass moments of inertia to be accelerated by the mechanical drive train.
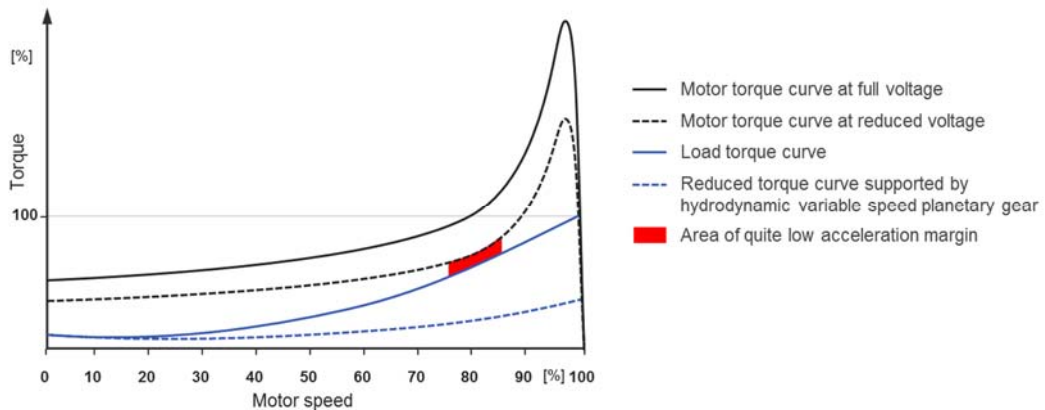

Figure 5 Squirrel cage induction motor capability curve at different voltage levels and load torque curve

The motor torque being available reduces with a square with the residual voltage caused by the voltage dip occurring during start-up. For a residual voltage level of 80 % for instance, only a motor torque of 64 % is still available: $T \sim U^2$. It therefore needs to be ensured during the projecting phase, for example by simulations that the counter-torque is always below the motor characteristic curve in order to achieve a torque reserve for the acceleration. In addition, a safety distance needs to be provided to consider spreading and to enable

a fast motor run-up. API requires a torque margin of 10% based on motor rated torque. On account of the thermal load, it is important to consider longer motor run-ups in the motor design.
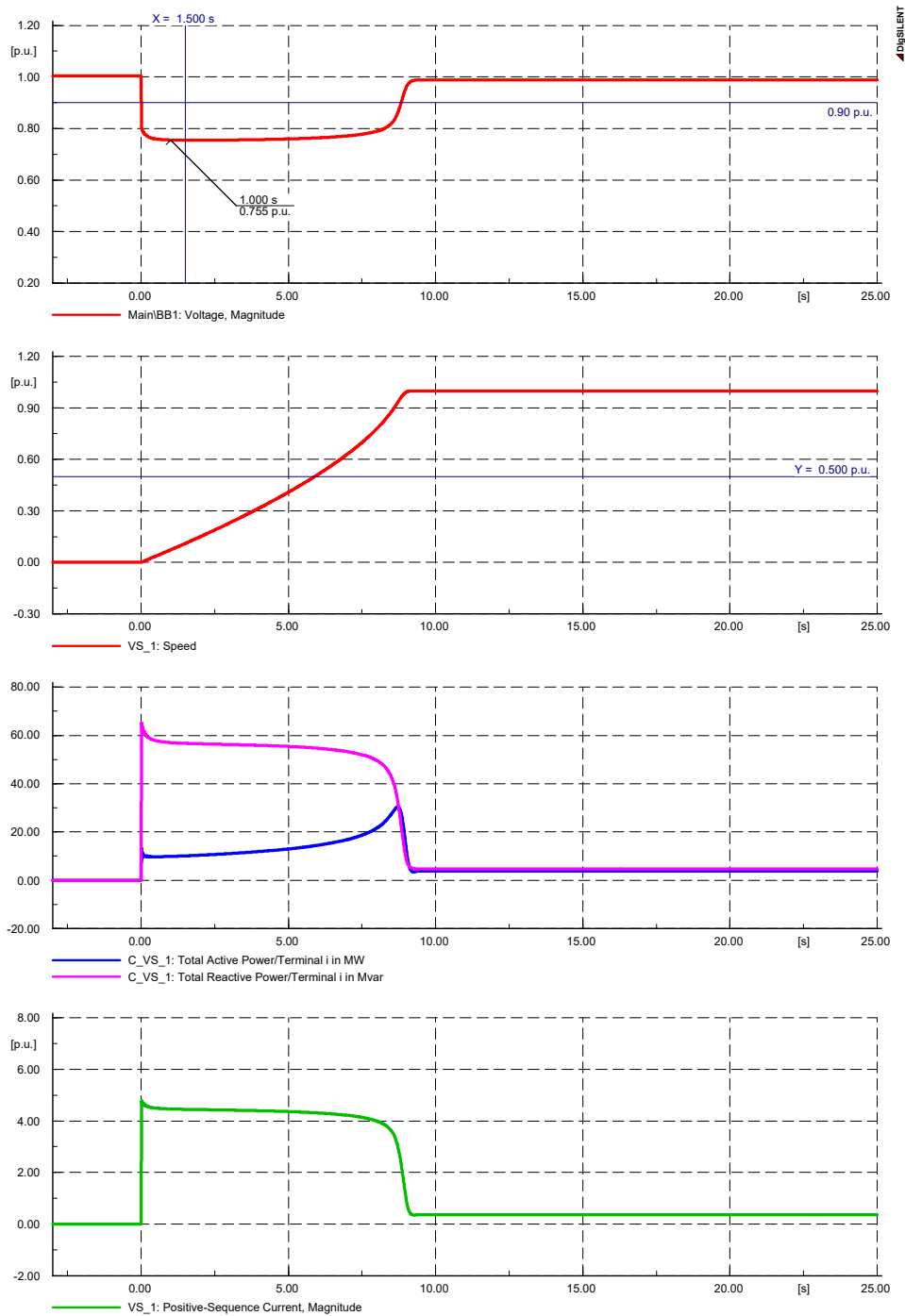

Figure 6 Direct online start-up of 15MW squirrel cage induction motor

It is always advantageous to reduce the relevant mass moments of inertia on start-up and the counter-torque of the compressor. This can be achieved in different ways, for instance, directly by a suction throttle or by a hydrodynamic variable speed planetary gear drive system (VHSD) whereby the load curve can be reduced significantly.

Figure 6 shows the starting course of a 15 MW motor. On account of the direct motor start with the grid configuration taken as basis, a maximum voltage dip of 25 % will result at the main busbar (Main / BB1) which in some applications will no longer be acceptable. The motor has a locked rotor current of 600 % but is reduced to 500% because of the dominate voltage dip. The motor run-up time will increase by the voltage dip. Nevertheless by using a VSHD drive system, the drive train will reach rated speed already after 9 seconds as the resulting counter-torque was reduced to 40 % when the motor had run-up. The counter-torque can also be reduced to about 7 % when using another gear type.

The required reactive-power absorption of the motor will be above the active power input by up to factor 6. Contrary to the active power, the reactive power will not result in a mechanical power conversion to the motor runner but is in this case mainly responsible for the voltage dip.

LIC - LOW INRUSH CURRENT MOTOR

Using a low inrush current motor (LIC), as shown in Figure 7, it is possible very simply and effectively to limit the current consumption while the motor runs up .
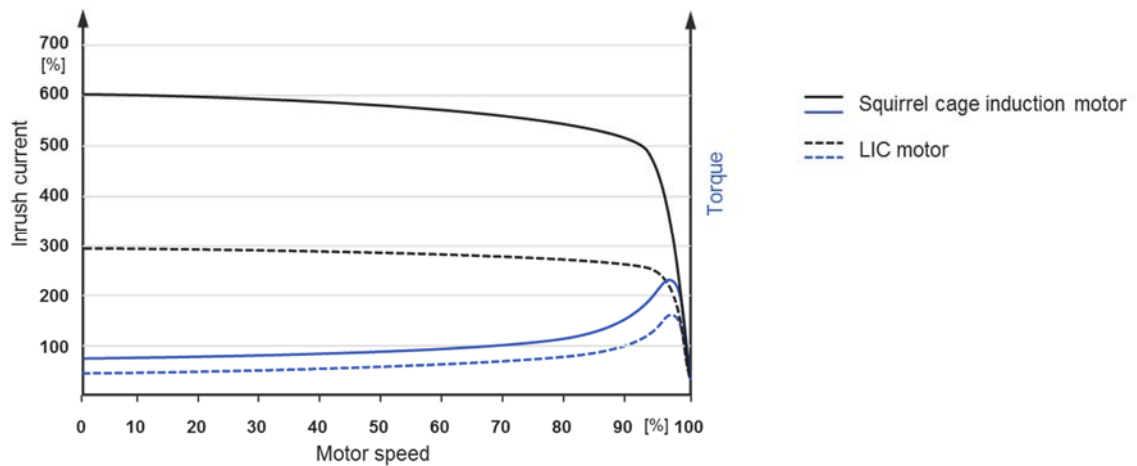

Figure 7 Comparison capability curve of squirrel cage induction motor vs. LIC motor

The maximum current consumption during start-up can be reduced to values which are three times the rated current by changing the rotor design. This will reduce the torque characteristic curve of the motor, and needs therefore to be considered in the projecting phase. The size of the motor will change only insignificantly. For many applications, cost savings for the transformers and energy generating systems in isolated networks are enabled by the use of LIC motors.

In the following illustration, Figure 8, the effects of this motor are depicted. The voltage dip will reduce to almost half compared to the conventional motor design. Whereas the motor run-up time will double to about 20 seconds, but is still clearly within the basic design. The stator is identical to the conventional squirrel-cage motor. The relation between reactive- and active-power input remains almost the same. Dependent on the variation of short-circuit capacity, this constructional measure may already be sufficient in a variety of applications to reach the connection conditions to power supply.

A further reduction of the starting current would basically be possible, however, it could result in a considerable increase of the motor mass and reduction of the efficiency, and will therefore be no longer economical. The relation between the reactive- and active-power input remains almost comparable to the conventional squirrel-cage motor.

Pros: - Very effective and economical possibility to reduce the starting current
             - Simple solution without effect worth mentioning on the footprints
             - moderate higher price than regular induction motor

Cons: - The max. current limitation is at approx. 300%, whereby the voltage dip cannot be reduced arbitrarily.
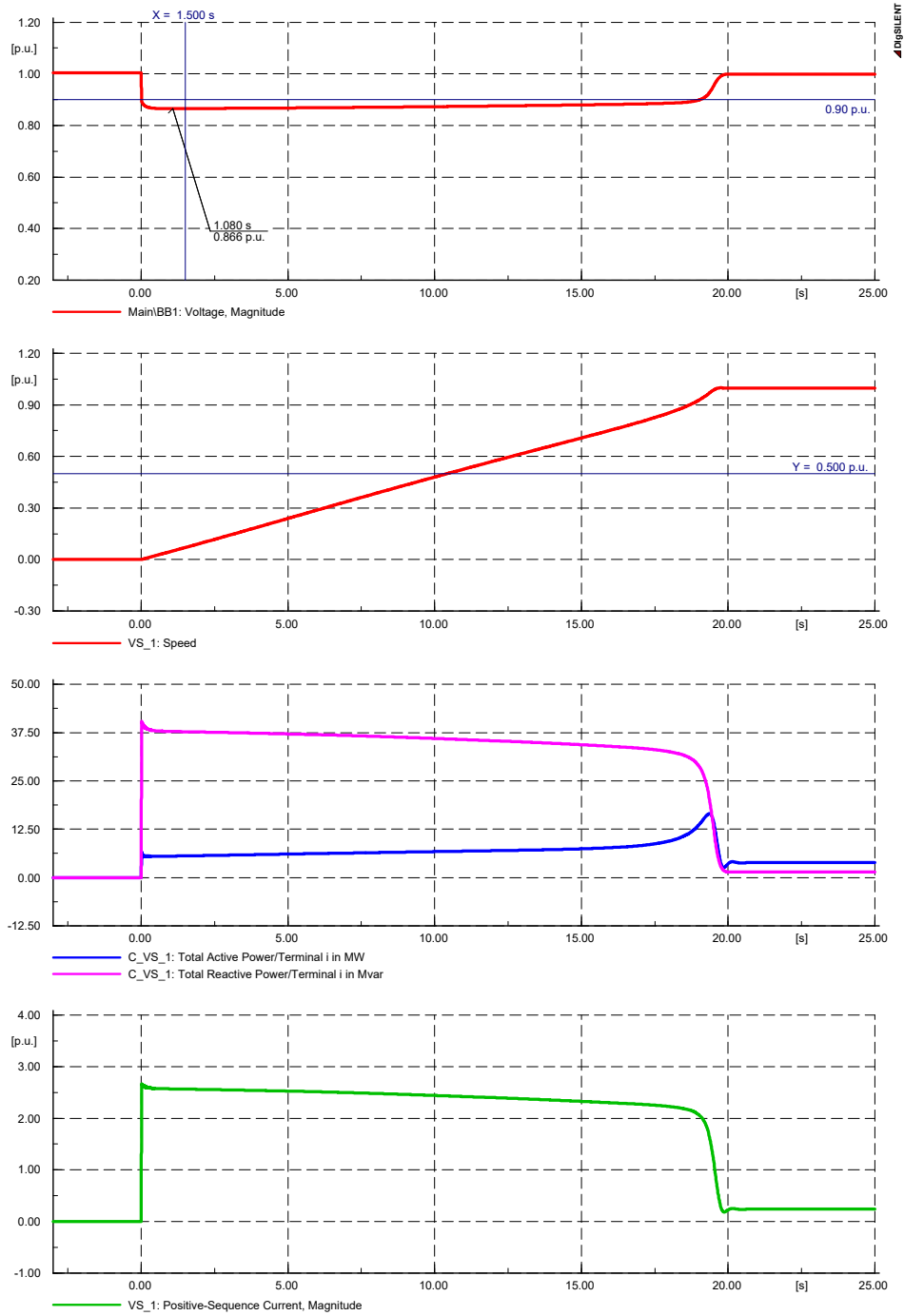

Figure 8 Direct online start-up of 15MW LIC squirrel cage induction motor

ROTOR RESISTANCE STARTING

Rotor resistance starting is a proven starting method for applications where a low short-circuit capacity relative to the motor power is present, and thus high voltage dips are to be expected. Moreover, this is preferred for heavy start-ups. In the past years, this starting method was replaced increasingly by VFD drives, especially in the medium and low power range.

The motor is provided with slip rings, which are connected to the runner that is designed as wound-rotor type. The stator is equivalent to the squirrel-cage motor. The slip rings are connected to power resistors, one per phase. This enables considerably to reduce the starting current. The resistance value is permanently reduced while the motor runs up. After the motor has run up, the runner connections are short-circuited inducing an operating behavior as for a squirrel-cage motor.

As depicted in Figure 9, the pullout torque can be moved to low speed by varying the resistance value whereby clearly higher starting torques can be achieved than with squirrel-cage motors.
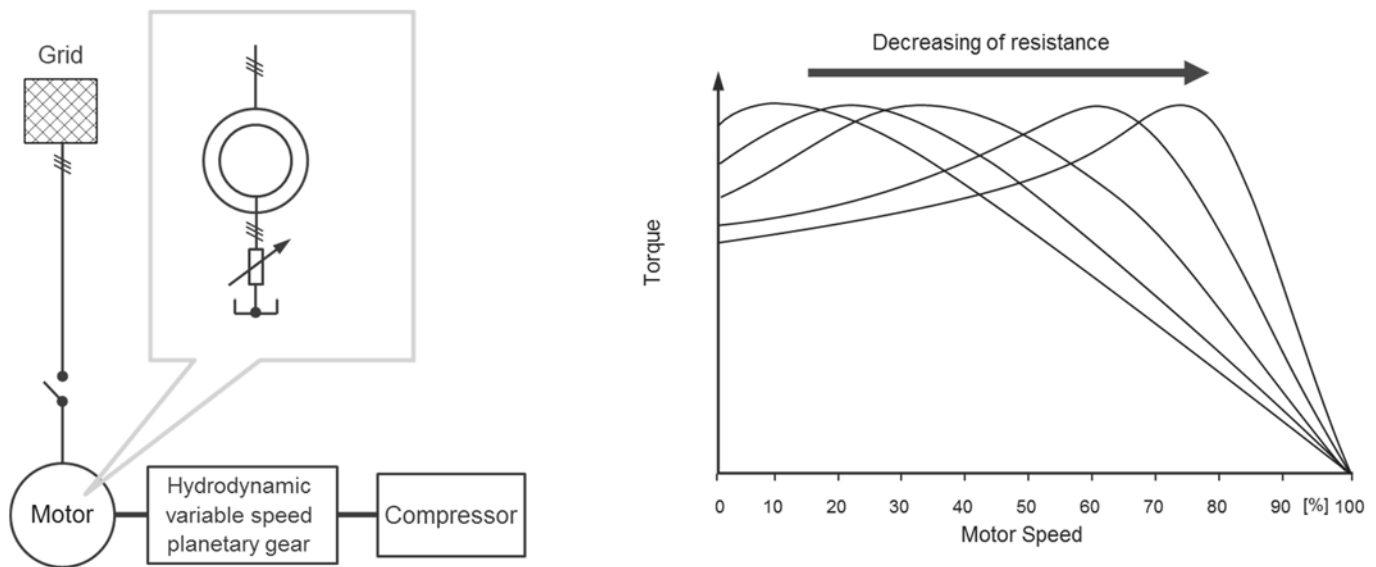

Figure 9 Layout of wound-rotor induction motor with additional rotor resistance

To apply a possibly high starting torque throughout the whole run-up process, the resistance is reduced as a function of the speed: R f(n), as realized in the simulation diagrams in Figure 10. The reactive power portion is reduced considerably by the power resistance and is just approx. 7% of the squirrel-cage motor's reactive power. In spite of the very high starting torque, the power consumption is lower than the rated current. A voltage dip of about 1% results which can be neglected.

Slip rings require an increased maintenance expenditure. Therefore, normally a brush lifting device is used if the slip-ring motor is used for starting only. This allows to considerably reduce the maintenance expenditure.

To vary the resistances, switchable, fixed resistors are used or a so-called liquid starter with an electrolyte where the resistances are infinitely variable. For fixed resistors, during the run-up, the resistances are varied via several stages. The simulation presents the liquid starter for which the change of resistance was simulated by a very fine grading of discrete resistances.

Pros: - High starting torque
           - Negligible circuit feedback and thus suitable for very weak grids
           - Proven and widely spread solution in industries beside turbomachinery
           - Soft start-up even in case of high loads or high break-away torque

Cons: - Motor is longer
           - Additional equipment is required for resistor starter
           - Suitable for solutions where start-ups are not frequently necessary
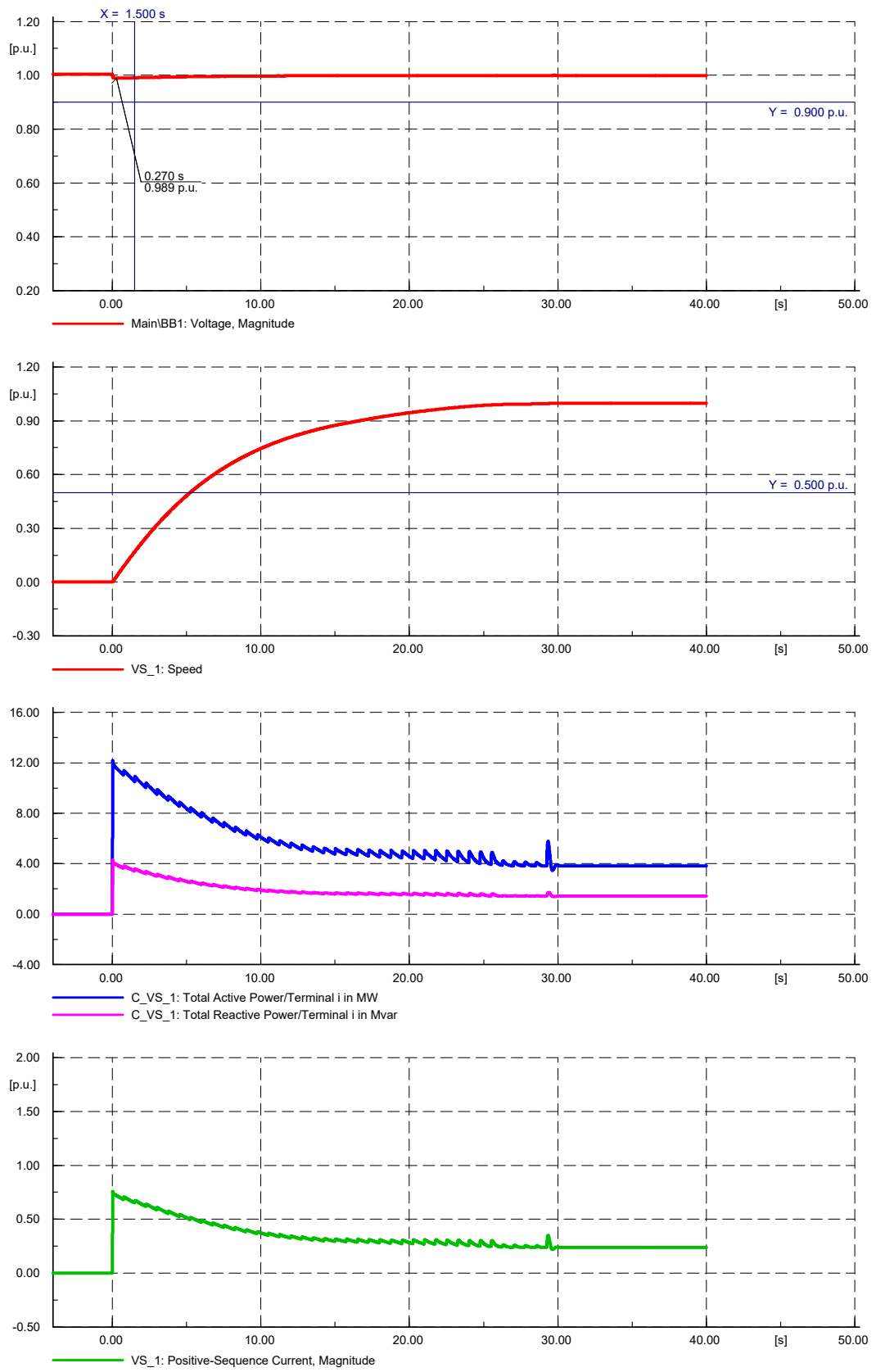   - Increased maintenance expenditure

Figure 10 Rotor-resistance starting of 15MW slip-ring motor

SOFT STARTER

For the soft starter, reverse-parallel connected thyristors are used which are arranged before the motor as depicted in Figure 11 . The current flow is controlled by the generalized phase control. This reduces the effective terminal voltage on the motor. After the run-up, the soft starter is bridged (s) and runs directly connected to the grid.
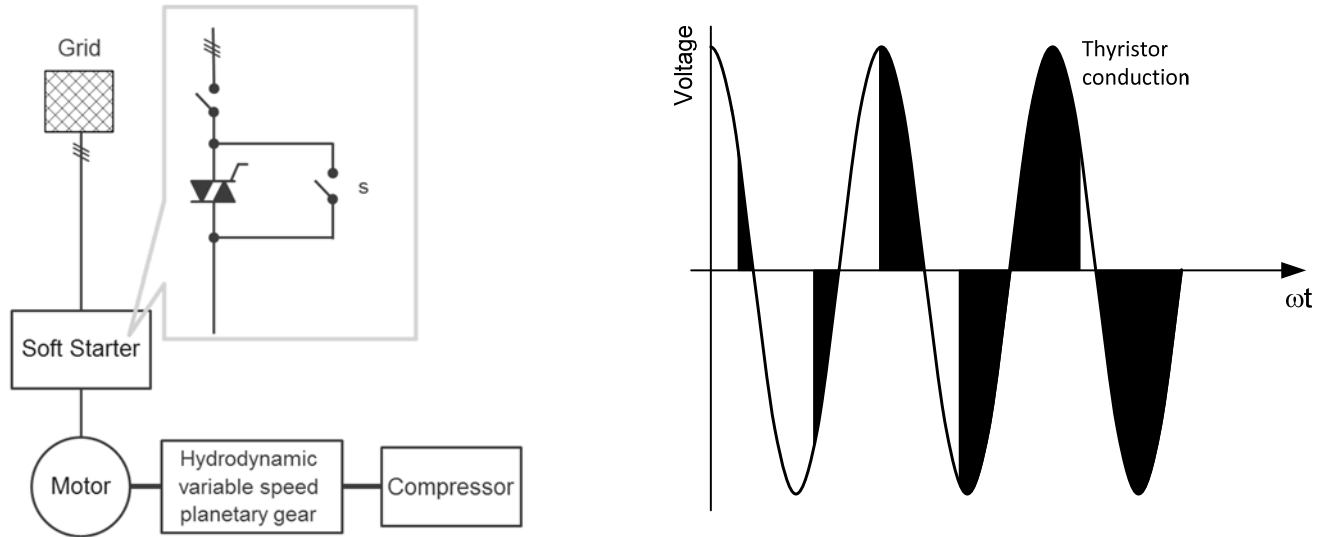

Figure 11 Motor with soft starter

Normally, the current limitation can be adjusted in the range from 100 .. 400 %.

The motor torque reduces with the square while the current flow reduces: $T \sim I^2$. In drive trains where the counter torque cannot be significantly reduced for the run-up, the current limitation can be reduced moderately only in order to ensure the reliable motor run-up. Thus, the voltage dip cannot be reduced arbitrarily. Figure 12 shows the start-up with a current limitation to 200%. The voltage drop will be limited to 90%. The reduced motor torque entails a run-up time of approx. 30 sec. With this method, basically a higher scope for action is achieved compared to the LIC motor as the max. current flow can still be readjusted during commissioning. However, the relation of the reactive- to the active-power input increases, even if only moderately, compared to the conventional and LIC motor whereas the influence of the reactive-power portion on the voltage dip increases. However, significant harmonic distortions are generated by the phase control. In some cases it may be necessary to install harmonic filters.

Pros: - Proven & tested many times
           - Starting current can be adjusted during commissioning

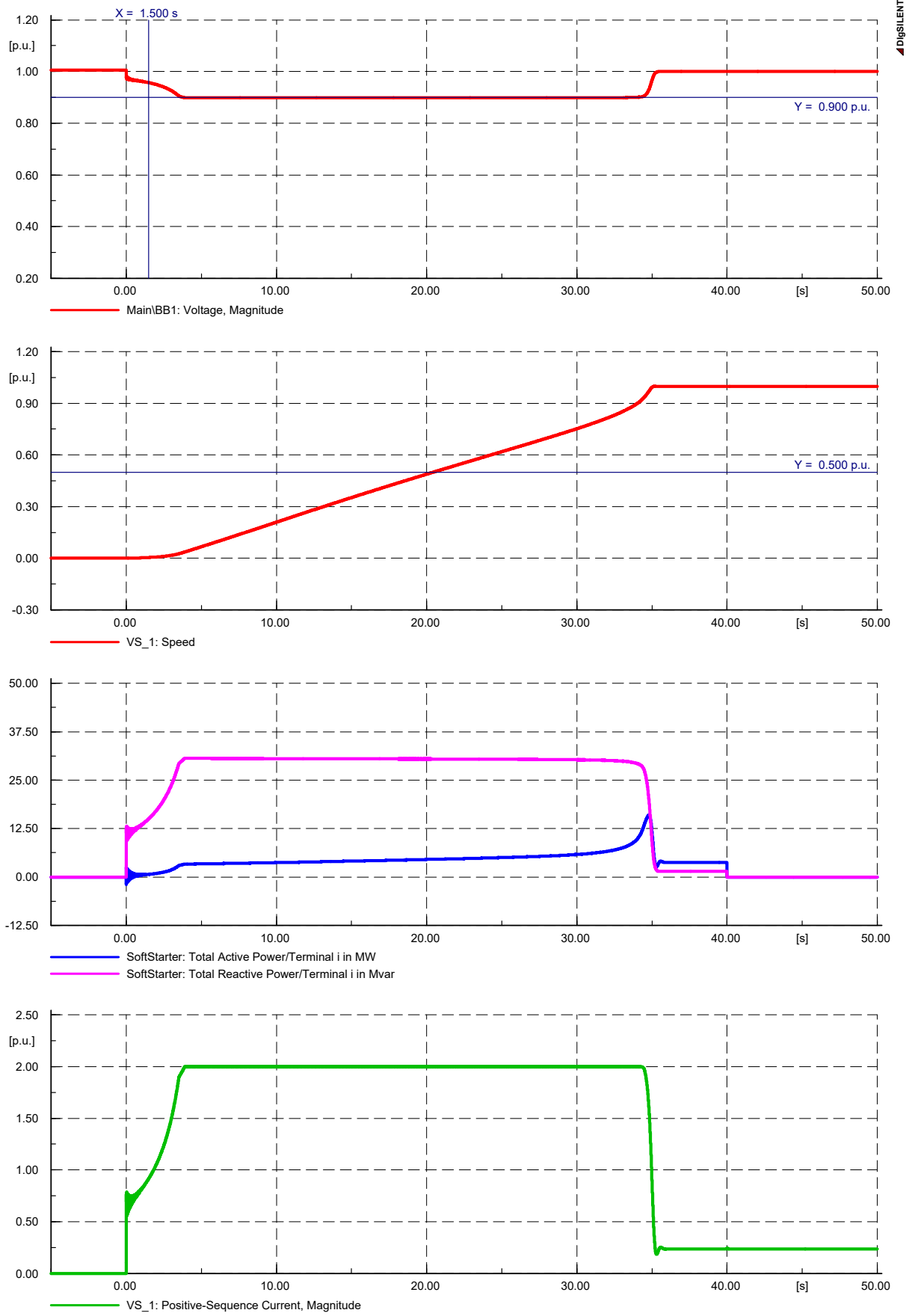Cons: - Generation of harmonic distortions while the motor runs up

Figure 12 Soft starter starting of 15 MW squirrel cage induction motor

Copyright© 2017 by Turbomachinery Laboratory, Texas A&M Engineering Experiment Station

AUTOTRANSFORMER

An autotransformer is similar to an electrical transformer with only one winding per phase. The windings are used likewise for primary and secondary side. Compared to this, an electrical transformer has a primary and an electrical isolated secondary winding which results in a higher weight and footprint.

The voltage ratio is reached by taps on the secondary side for the motor circuit, at least three taps are required in all. The voltage ratio can be adjusted by using additional taps.

The autotransformer has two starting stages before reaching normal operation in Step 3:

1. The Star switch 3 is closed before main switch 1 is enabled. The autotransformer operates as a voltage transformer.

2. After reaching a predetermined speed the Star switch 3 is opened. The autotransformer acts as a reactor.

3. After reaching close to rated speed the main contactor switch 2 is closed. The autotransformer is bypassed and start-up procedure is finished.
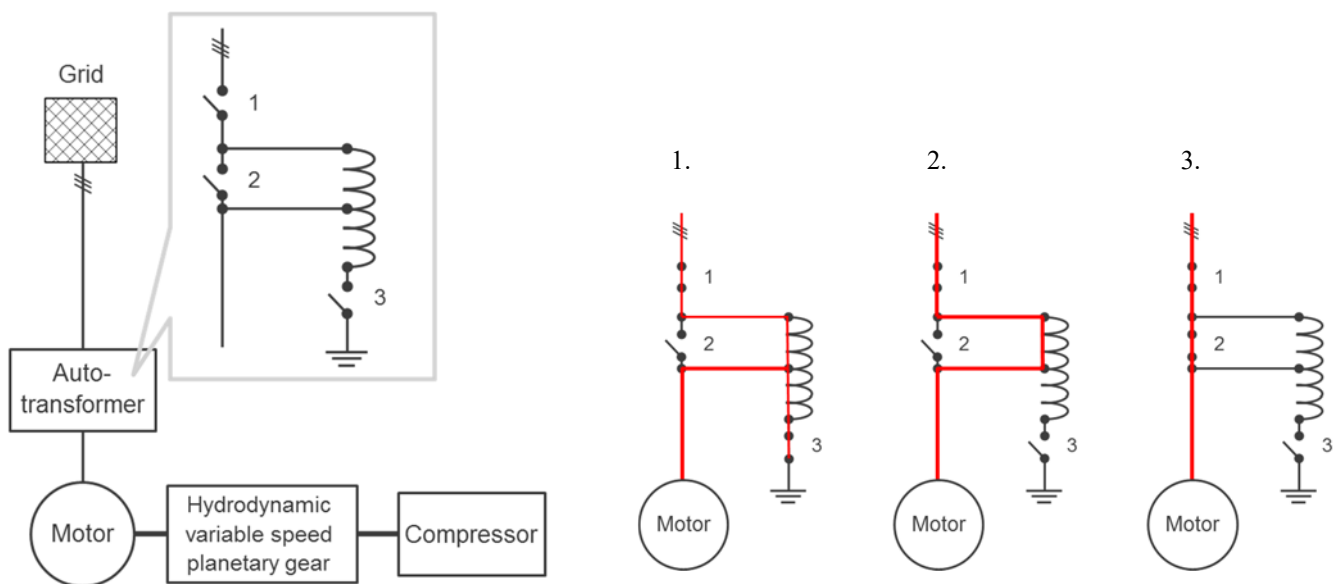

Figure 13 Motor with autotransformer

Figure 14 shows the starting response of the 15 MW motor. In this case the star switch is opened when the motor reaches 60% of nominal speed The bypass switch is closed one minute after starting. The secondary winding tap was set to a voltage ratio of 0.85 which is 9.4 kV. The switchover of the different starting sequences is uninterruptible. The 2nd stage, where the autotransformer operates as a reactor leads to a higher reactive power amount, resulting in an additional voltage dip on the busbar. In general the reactive power related to active power consumption is comparable to a soft starter. In this example the inrush current is limited to approximately 150%.

Pros: - Multiple proved technology
   - Voltage adjustment by using of additional taps
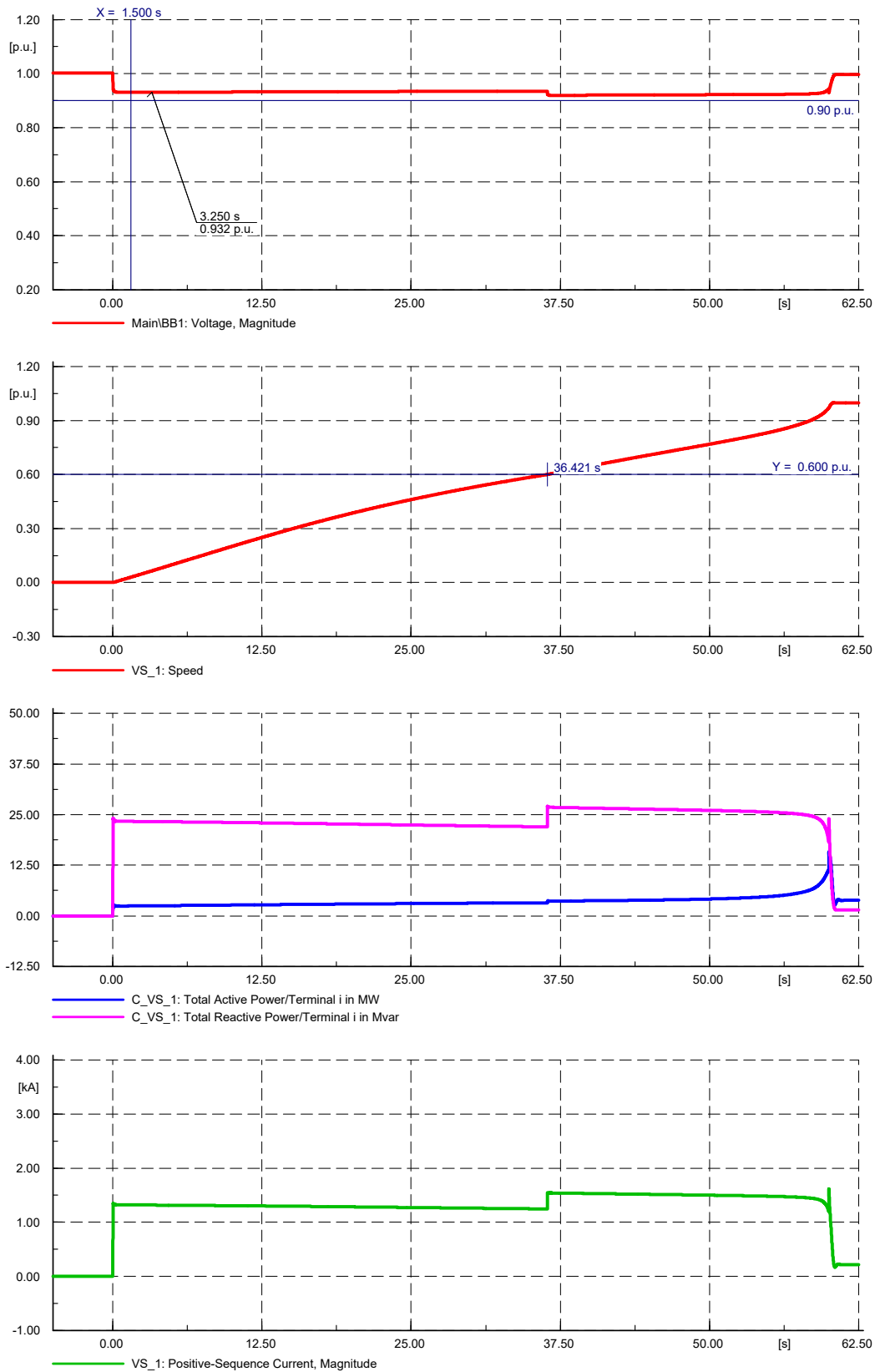
Cons: - 3 contactors are needed

Figure 14 Autotransformer starting of 15 MW motor

Copyright© 2017 by Turbomachinery Laboratory, Texas A&M Engineering Experiment Station

PONY MOTOR STARTING

Pony motor starting is used for high main motor power because the above mentioned start-up methods becomes insufficient regarding avoidance of high voltage dip and grid disturbances. As shown in Figure 15, a 24MW synchronous main motor is started using a 2MW pony motor and a torque converter. Instead of a torque converter a VFD driven pony motor can also be used.
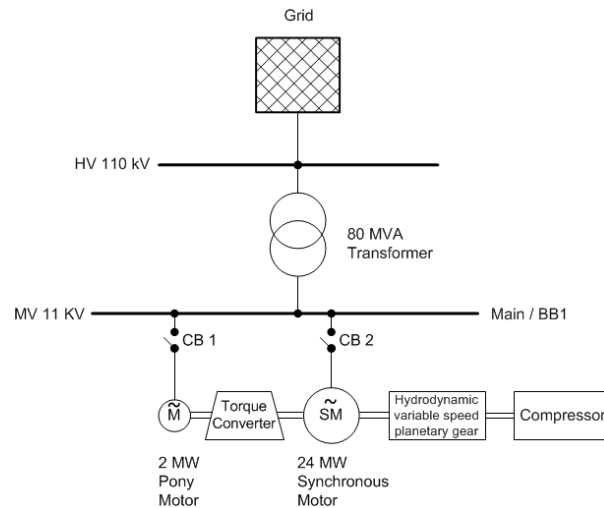
Figure 15 Power Supply - Single line diagram for 2MW pony motor starting of 24 MW synchronous motor

The torque converter can disengage and allows for the load-free starting of the pony motor and a smooth and controlled run-up of the synchronous motor [6]. The main steps of the starting process are as follows:

1. Close circuit breaker CB1 to run-up the pony motor.

2. Run up the synchronous motor using the pony motor and the torque converter.

3. Switch on the excitation system.

4. Synchronise the motor with the main power supply by controlling its voltage, speed (frequency) and phase angle.

5. Close the main circuit breaker CB2. No inrush current occurs.

Following the successful starting of the motor the VHSD drive system runs up the mechanical load and regulates its speed to the value required by the compressor. This grid does not notice a visible voltage dip.

The simulation of starting the synchronous motor includes the entire process, from starting the pony motor to synchronising and connecting the synchronous motor to the grid.

The industrial power system in Figure 15 is supplied from an 110kV network by an 80MVA transformer. The 110kV network has a short-circuit level of 10kA and the 110/11kV transformer has a short-circuit impedance of 14%. The study was performed for a 50Hz gird. But the results are also applicable for 60 Hz.

The synchronous motor is modelled as per IEEE recommendations [2], [3], [5]. The model includes the equations for two rotor circuits in both the direct axis and the quadrate axis, saturation of the stator core and a single-mass shaft. The shaft equation includes the inertia of the motor's shaft, the inertia of the torque converter's secondary side, the inertia of the VHSD's primary side and coupling elements. Figure 16 lists the motor's main parameters.

The excitation system of the synchronous motor has been modelled as a PI-regulator, which regulates terminal voltage. In practice the excitation system would include further functions (such as under- and over-excitation limiters and reactive power regulator). These, however, are not required for the studies presented here.

The pony motor is represented by a standard asynchronous model [2], [3], which includes the equations for two rotor cages with constant parameters and a single-mass shaft. The inertia includes that of the motor and the torque converter's primary side. Figure 16 lists the main parameters of the pony motor.

The efficiency of the torque converter is assumed to be 80% throughout its operating range. This simplification has a negligible impact on the steady-state power drawn by the pony motor.

Parameter	Synchronous motor	Pony motor
Rated mechanical power	24 MW	2 MW
Rated voltage	11 kV	11 kV
Rated power factor	1.0	0.91
Rated speed	1500 rpm	-
Nominal speed	-	2991 rpm
Inertia	3294 kgm² (including motor, VSHD primary side)	83.7 kgm²
Locked rotor current	-	5.0 p.u.

Figure 16 Main parameters, synchronous and pony motor

The counter-torque of the unloaded VSHD drive system shown in Figure 17 has been considered for the run-up of the synchronous motor, which requires only 5% at rated speed. Later, when the motor is synchronised and the VSHD runs up to operating range, its counter-torque will depend on the loading of the mechanical load.
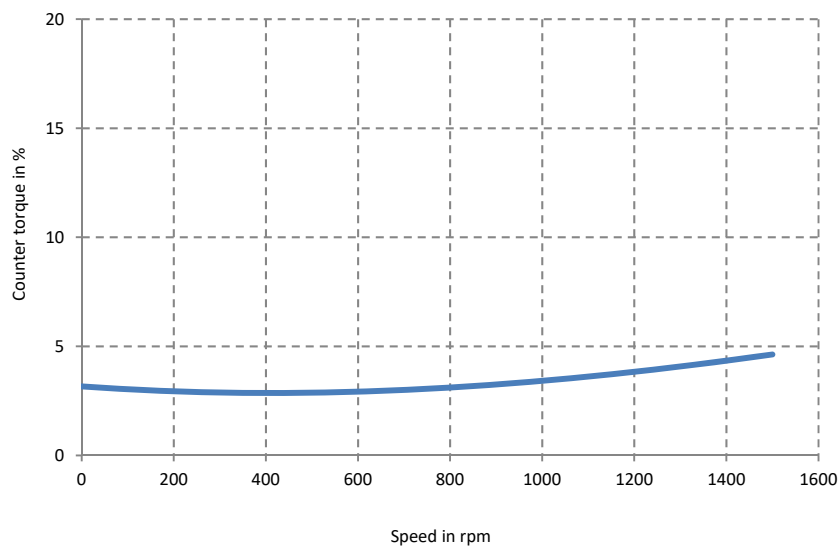
Figure 17 Counter-torque of unloaded VSHD drive system

Pony motor starting

The transient response during the starting of the pony motor is shown in Figure 18. The pony motor draws a reactive power of approximately five times its rated power, leading to a voltage dip of some 2.5% at the 11kV busbar. The pony motor runs up within about 6.5s, after which time the voltage at the 11kV busbar recovers to within 0.3% of the initial value. As it reaches its final speed there is a small oscillation since its speed initially overshoots the final speed.
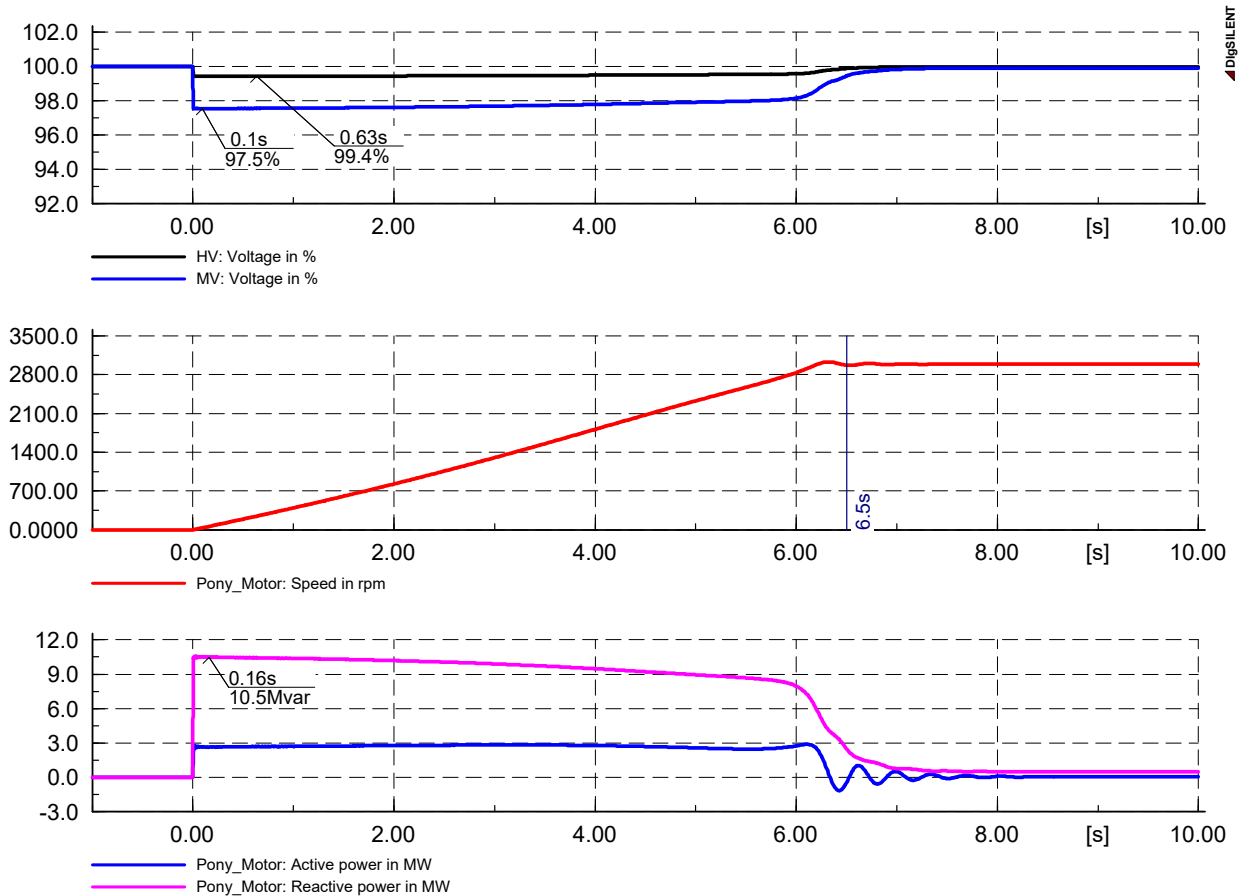

Figure 18 2 MW Pony motor starting

Synchronous motor run-up

Following the starting of the pony motor, the torque converter is activated to transmit torque to the synchronous machine – see Figure 19. The torque is initially limited to $M_{max} = 5\%$ of rated synchronous motor torque (this could be increased to reduce the run-up time).

The motor runs up in some 260s, after which the speed is regulated to a value marginally above the frequency of the external power system. In this case the speed has been regulated to 1501.5 rpm. The pony motor draws a maximum power of 1.6 MW whilst it accelerates the synchronous motor. The maximum voltage depression at the 11kV busbar is some 0.2%.
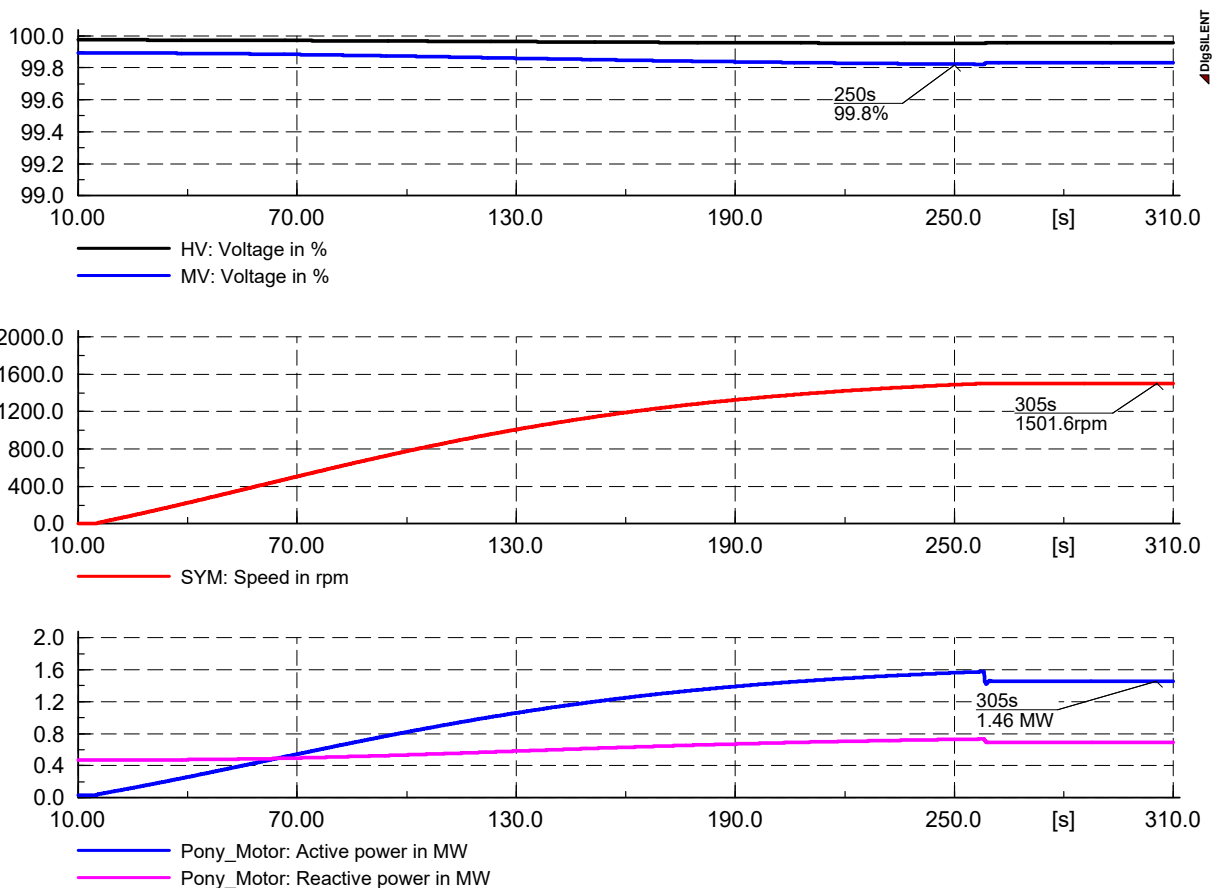
Figure 19 Synchronous motor run-up

Following the successful starting of the synchronous motor the pony motor consumes about 1.5MW. The mechanical load is at standstill and is only started later, after the synchronous motor has been connected to the grid.

Synchronizing

Following the acceleration of the synchronous motor its excitation system is switched on. This process has been simulated at a time of 300s after the closing of the pony motor's breaker CB1. The response of the terminal voltage is shown in Figure 20. In reality, the voltage regulator can be tuned to achieve a response time of between about 200ms and some seconds. The only constraints are that the maximum rotor current should not be exceeded (the limit is typically about 250-300% of the value required in open circuit when neglecting saturation) and that any overshoots should be below the protection trip value (typically about 120%).

The set-point of the voltage is determined by an automatic synchronising device and set to equal the voltage at the 11kV busbar within a small tolerance (typically about 2%). In this case the voltage was regulated to 100% whilst the voltage at the 11kV busbar was 99.8%.
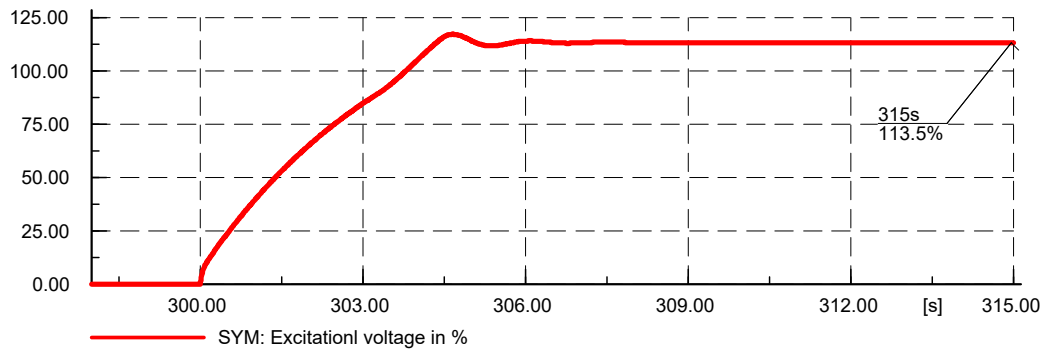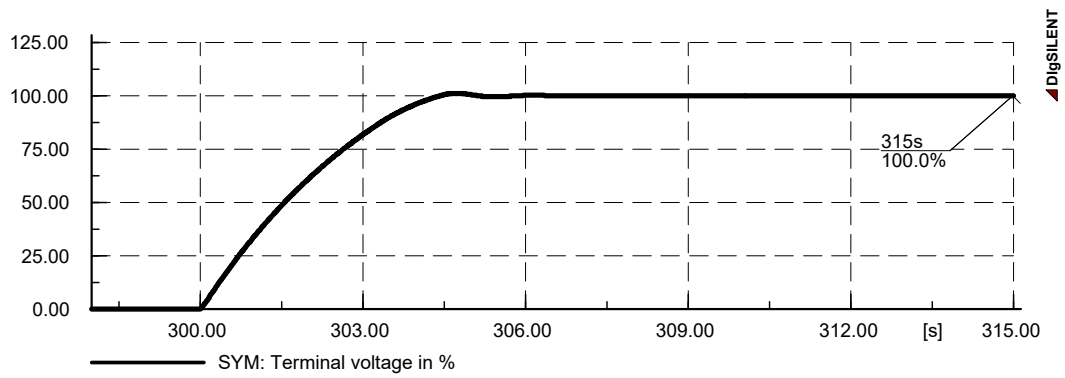
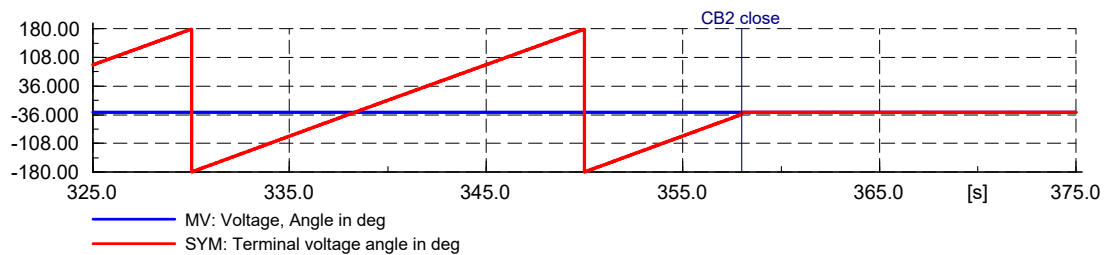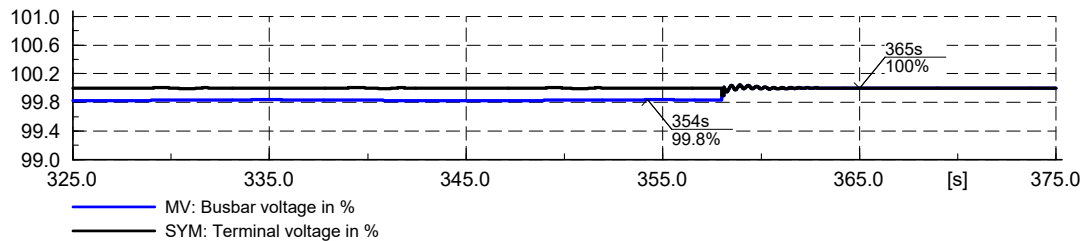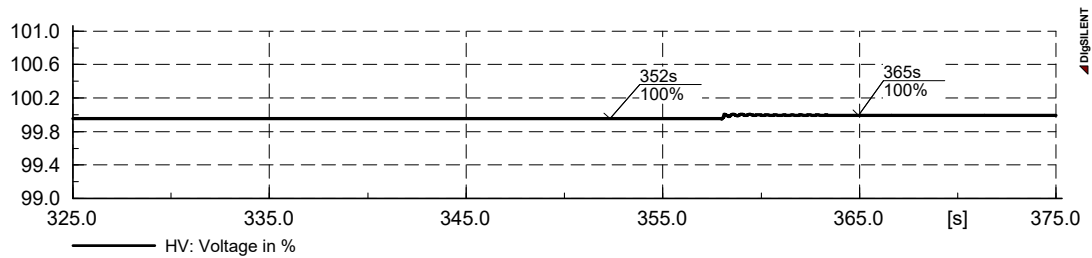**Figure 20 Switching on excitation**

Figure 21 Voltage response during synchronization

Figures 21 and 22 show the response during the synchronisation of the generator to 11kV busbar and the closing of the breaker CB2. Synchronising requires the voltage magnitude, voltage phase angle and frequency of the generator to be matched to those at the 11kV busbar. The voltage magnitude is set through the voltage regulator and the frequency through the speed controller. By setting the frequency to be marginally different to that at the busbar the motor's phase angle continues to vary relative to that of the busbar and the breaker can be closed when the phase difference is approximately zero.

The circuit breaker CB2 has been closed at the simulation time 358s. The resulting transient depends on how closely the generator voltage, phase angle and frequency are matched to those of the 11kV busbar prior to the closing. These parameters, in turn, are adjustable in the automatic synchronizing controller. In this case the voltage change at both the HV busbar and the 11kV busbar was less than 0.5%.
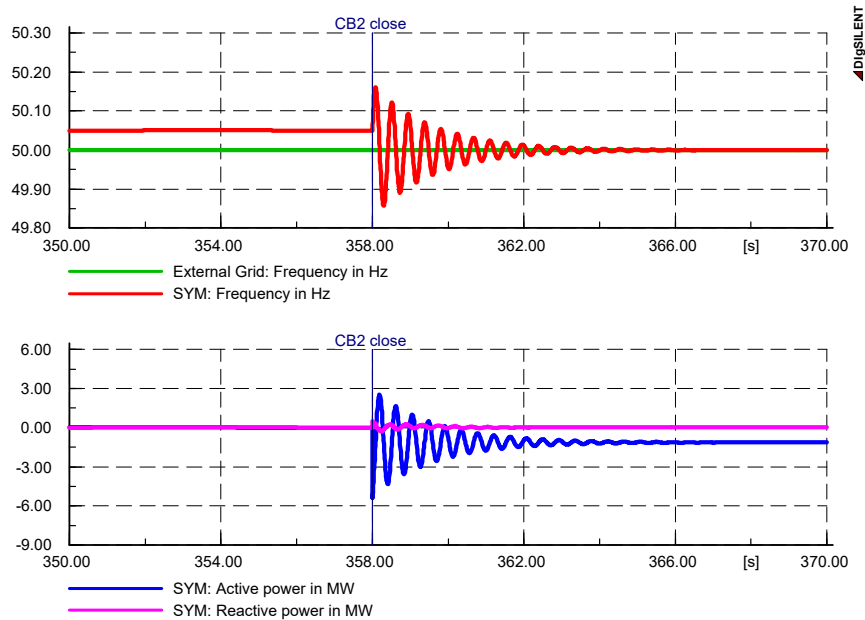

Figure 22 Speed response during synchronisation

The response also includes a well-damped oscillation of the synchronous motor's shaft. The frequency of oscillation depends mainly on the inertia and the supply impedance. In this case the frequency is some 2.5Hz. The final speed corresponds with the frequency of the external power system (1500rpm for 50.0Hz).

After the synchronous motor is connected to the power grid, the pony motor trips immediately (e.g. 100ms), the torque converter is drained and the pony motor runs down. The motor's starting process is then complete and the drive is ready to start the mechanical load.

Pros: - Grid disturbance of pony motor starting is minor
            - Smooth run-up and synchronization of main motor
            - Preferred for huge motor power and weak power grid

Cons: - Increased installation length

Summary

Five frequently used starting methods were presented:

1. Low inrush current motor
2. Rotor resistance starting
3. Soft starter
4. Autotransformer
5. Pony motor starting

Comparison of starting methods is mainly concentrated on the technical differentiation. There is no solution that is reasonable for all situations. In fact, the individual requirements and the achievement of the objectives are important. The consideration of capital and

operational expenditures was deliberately not discussed as these expenditures depend on many factors and cannot be generalized.

The simplest and most economical possibility is the low inrush current motor for which the starting current can be reduced effectively but not arbitrarily by a change of the design of the runner of a squirrel cage induction motor. On account of that, the LIC motor is preferably used wherever a mean short-circuit power exists compared to the motor power.

The slip-ring motor is provided with an installed but variable power resistance to limit the starting current. It is characterized by a high starting current. The voltage dip can be neglected. The slip-ring is only in contact during start-up by a lifting device reducing clearly the maintenance intensity. It is suitable for very weak grids.

The soft starter provides a widely spread method to reduce the starting current by phase control and thus the effective voltage. Partly harmonic filters are used to avoid harmonic distortions. The soft starter is suitable for mean short-circuit powers, and may also be used for weak grids if the counter torque can be reduced in the run-up phase.

For an autotransformer, the voltage is reduced directly by a tapping. Effectiveness and usability are comparable with the soft starter.

Pony motor starting is preferred for very large motors and very weak grids. The pony motor which has a power consumption of approx. 8 % of the main motor run-ups this to rated speed. Voltage dip for the direct online start-up of the pony motor is minimal. When using a synchronous main motor, low-harmonic grid synchronization can be achieved and a voltage control during operation. In case of short-circuit, the motor acts inherently grid-supporting by the subtransient reactances.

ELECTRIC-MOTOR-DRIVEN COMPRESSION AND TRAIN CONSIDERATIONS

End-users of Electric Motor-driven gas compressor (EMD-CS) applications demand high availability and durability. Equipment providers are acutely sensitive to this in product design, construction and packaging for site operation.
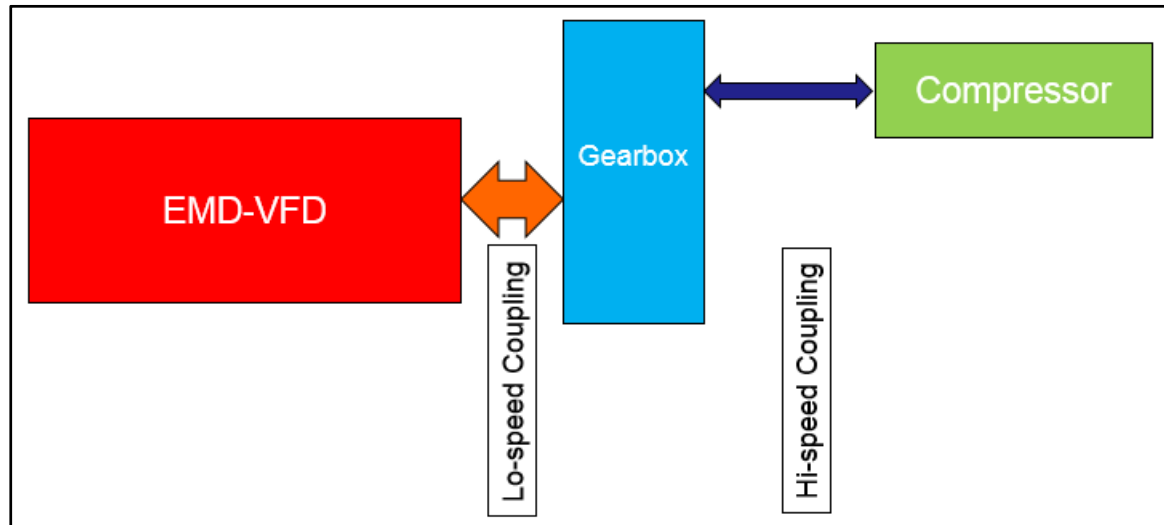

Figure 23 Typical train configuration of an Electric Motor driven Compressor package

One area of concern with Electric-Motor-driven compressor solutions has been the train's torsional characteristics. Torsional vibrations are an important consideration in EMD-CS packages due to the integration of components that have vastly different inertia and stiffness characteristics. Unlike turbine-driven compressors, EM-driven compressors can be subject to large air-gap torque pulsations and fault-event transients; these are serious conditions that must be endured by robust mechanical design of the train equipment. While a vast majority of EMD-CS installations provide trouble-free operation, there have been many examples of failures related to torsional vibration – as reported by the end-users in the literature [7]: broken gear teeth, coupling failures, fatigue effects or plastic deformation in driven equipment shafts etc. End-users have mandated due-diligence on train's torsional integrity from the OEMs.

TRAIN TORSIONAL INTEGRITY

The topic of train torsional integrity deals with the torsional natural resonances, their interference with operating speeds, sources of torsional excitation, type of excitation and most importantly, the ability of individual components in the train to handle the peak static and dynamic stresses within appropriate safety margins. Questions that need to be answered are:

- Are all the train equipment adequately designed to handle the torsional vibrations?
- Will the motor operation at rated conditions be acceptable to the driven equipment?
- Will the high speed couplings provide safe operation at all steady-state and transient conditions?
- Given the air-gap torque pulsations, are all the train equipment designed to meet "Infinite-Life" from Endurance standpoint?
- Ability of the train to handle high transient torque levels from motor fault events

Ascertaining torsional integrity of EMD-CS packages involve a series of analysis:

- Determining torsional natural frequencies (TNFs) and their interference on low-speed and high-speed shafts
- Steady-state harmonics from the VFD, subjecting the train to a forced response analysis and evaluating the resulting individual component stresses from a High Cycle Fatigue (HCF) standpoint
- Transient fault events (such as 2-Phase and 3-Phase short circuits), subjecting the train to transient torque through the fault time period, and confirming the resulting PU torque levels are within safety margins.

API and GMRC have long-recognized the need for providing appropriate torsional information and has outlined this in guidelines ([8], [9]). These guidelines are used extensively in the assumptions, analysis and data interpretation.

TORSIONAL SOLUTION METHODS

Many references exist in the literature in the torsional formulation and solution methods, so this paper will focus on the aspects relevant for interpretation of analytical results presented in later sections. The torsional analysis is performed by a Finite Element formulation of the train as branched systems (Figure 24), developed by one of the authors.
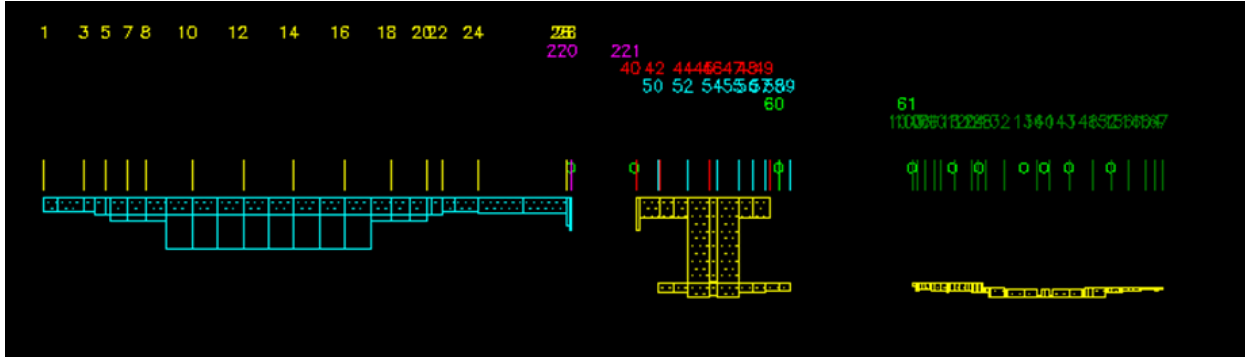

Figure 24 Torsional simulation model used for the Finite-element analysis

The twist in the shaft system (θ) can be represented as a harmonic function:

$$\theta = \theta_0 . \sin(\omega t)$$

where, θ_0 = Amplitude of the harmonic excitation, ω is the angular frequency and t, the time.

The equation of motions for the Finite Element formulation is written as:

$$[I]\{\ddot{\theta}\} + [C]\{\dot{\theta}\} + [K]\{\theta\} = \{f(t)\}$$

where

$[I]$ = Inertia matrix

$[C]$ = damping matrix

$[K]$ = stiffness matrix

$\{\theta\}$ = angular displacement vector

$\{\dot{\theta}\}$ = angular velocity vector = $\dfrac{\partial \theta}{\partial t}$

$\{\ddot{\theta}\}$ = angular acceleration vector = $\dfrac{\partial^2 \theta}{\partial t^2}$

$\{f(t)\}$ = Periodic or aperiodic forcing function vector

The element matrices are assembled into system inertia [I], damping [C] and stiffness [K] matrices.

The computer simulation tool accepts mass-elastic information of all the train components and the sources of torsional excitation. It then provides solution to the second order partial differential equation in the form of:

a) Steady-state solution: torsional vibration modes and responses
b) Damped response solution: torsional amplitudes for specific harmonic excitations, and
c) Transient response solution: torsional amplitudes for time-varying forcing functions. Time-marching methods, such as Runge-Kutta or Newmark-Beta, are used to perform direct time integration of the 2nd order differential equation. The fault transients arising from electric-motor (2-phase or 3-phase short circuits etc.) are analyzed with transient solution. Forcing functions are provided by the motor vendors, based on their drive and motor design. With the transient solution, the peak torque levels (PU) and the shear stresses at various components are calculated across the train.

Torque: $\{T\} = [K] . \{\theta\}$

Stress: $\{\sigma\} = \dfrac{\{T\}r}{J}$

Where, r = radius of the shaft element

J = polar moment of inertia of the element

TORSIONAL INTERFERENCE STUDY

The primary task in a torsional integrity study is to determine the train torsional resonances and review them against the desired operating speed range of both low-speed and high-speed shaft systems. In general, the first few (1 to 3) torsional resonances are most important due to the energy content in those modes and mode shapes. For sources of excitations, certain harmonic multiples of a) the train speeds (mechanical) and b) the VFD-output frequencies (electrical) must be considered for interference. The goal is to keep most prominent torsional interference with necessary separation margins; where interference is not avoided, the modes are shown to be safe from a torsional standpoint.

Figures 25 and 26 show the torsional interference charts (Campbell diagrams) with low-speed shaft as reference, for the train configuration mentioned earlier. One important source of excitation to consider with electric motors is the VFD harmonics transferred to the rotor through the air-gap. This information is provided by the motor vendor, and varies based on the VFD-type, Inverter design and number of voltage-cells. The fundamental VFD-induced excitation occurs at 6f, where f is the frequency output of the VFD. Additional multiples of this fundamental occur at 12f, 24f and 48f. For a 4-pole motor, these harmonics translate to 12X motor (6f), 24X motor (12f), 48X motor (24f) and so on, when plotted on the Campbell diagram. When the low-speed shaft is referenced, torsional interference occurs within the operating speed range (900-1890 rpm) between the following:

- 1st Torsional Resonance and 1X motor speed
- 2nd Torsional Resonance and 2X motor speed
- 2nd Torsional Resonance and 3X motor speed
- 3rd Torsional Resonance and 24X motor (12f VFD harmonic)
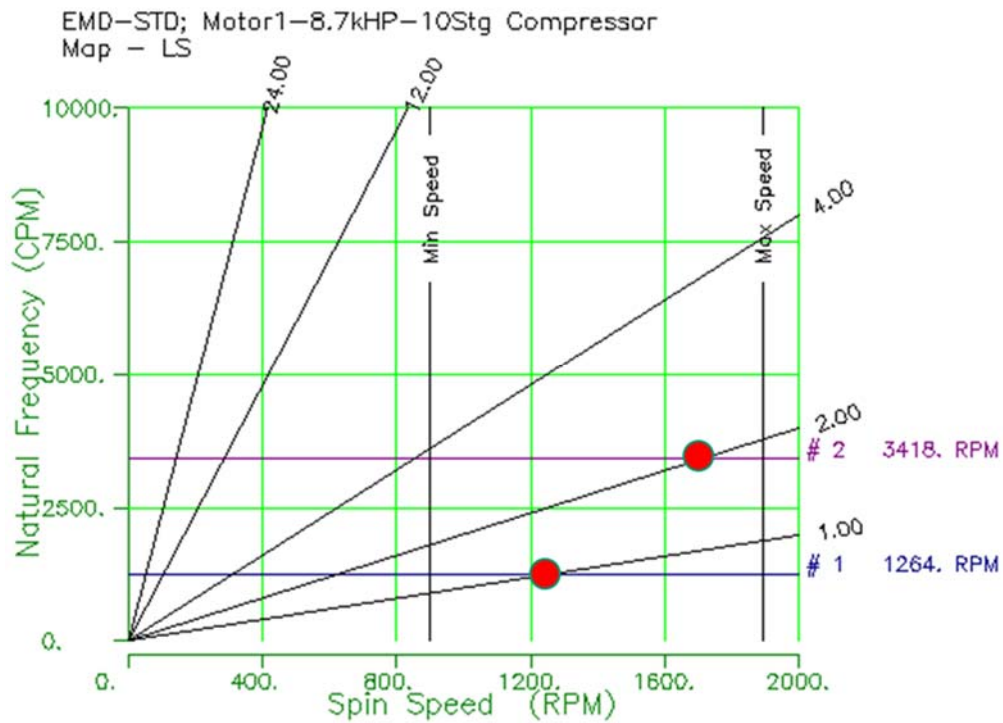- 4th Torsional Resonance and 24X motor (12f VFD harmonic)

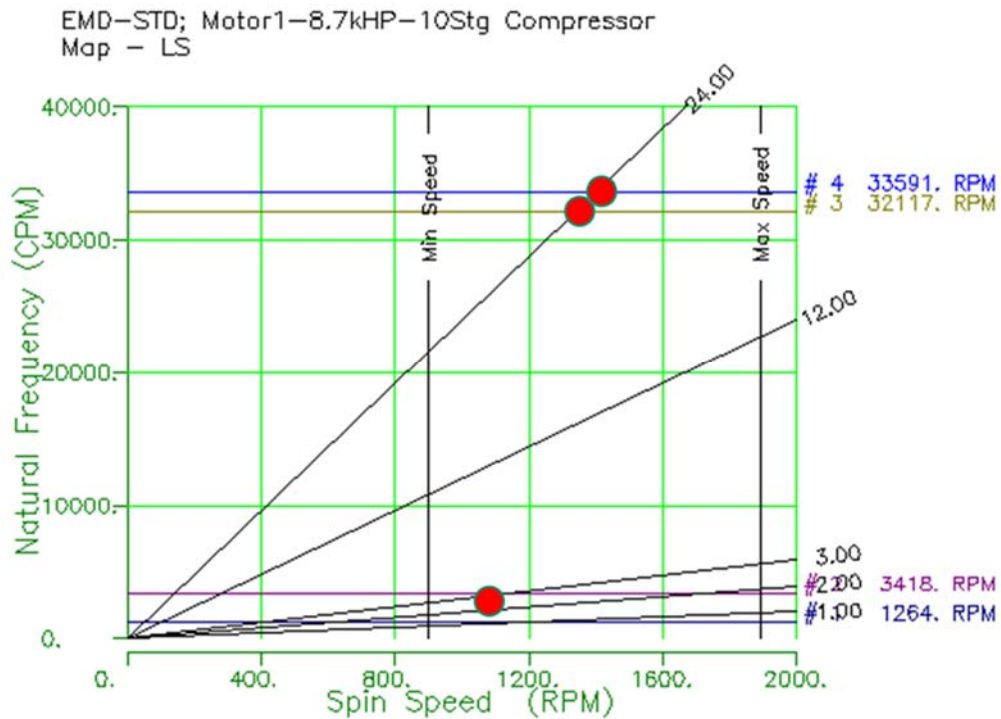**Figure 25 Torsional interference – Low Speed shaft as reference**

Figure 26 Continuation of torsional interference chart – Low speed shaft as reference
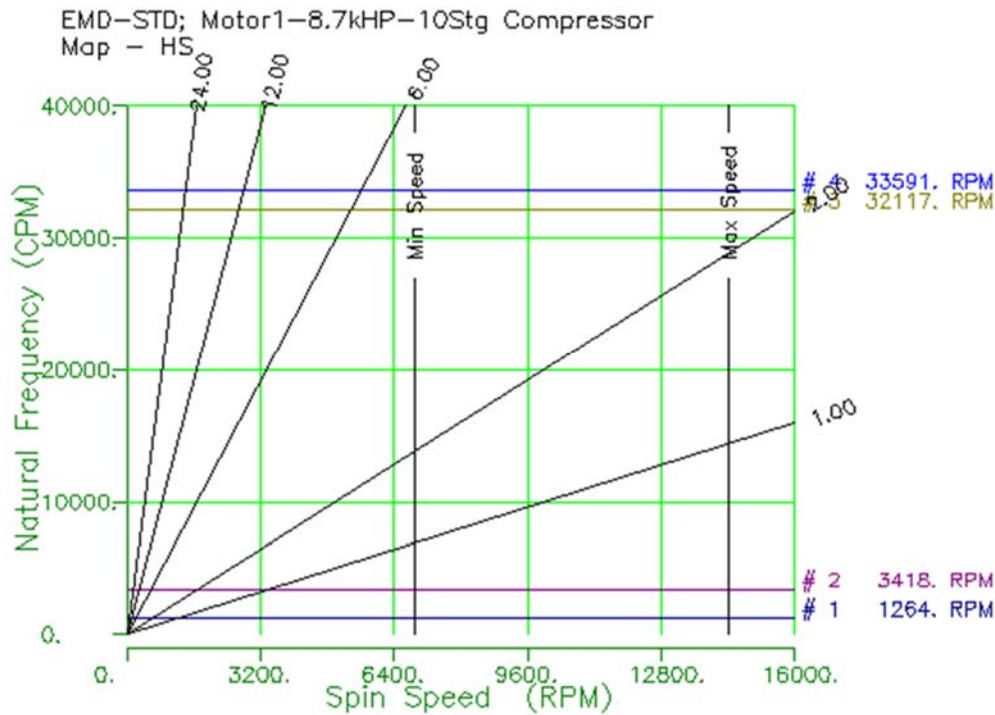
Figure 27 Torsional Interference chart – High speed shaft as reference

Figure 27 shows the torsional interference chart with high-speed shaft as reference. Note that there are no interferences between the lower-order torsional resonances and any significant excitation sources.

Altering train torsional frequencies to meet margins is not always possible, since any modifications to equipment must not violate other design norms. The softer stiffness elements in the train impact first few torsional modes strongly and hence, coupling designs are reconsidered whenever modifications are sought. However, coupling changes (length, type, weights etc.) can significantly impact package design and foot-print. Hence, it is best to incorporate coupling designs that can comfortably accommodate all technical requirements as well as equipment-access capabilities.

Based on the interference charts shown above, the low speed coupling design is optimized to provide the maximum separation margins and least torsional response at excitation (explained in the next section). Both the torsional stiffness (length and diameter) and inertia to a lesser extent were optimized.

STEADY-STATE HARMONICS & TORQUE PULSATION

As explained earlier, when torsional interference cannot be avoided with operating speeds, analysis must be done to prove that the train has low torsional response to the excitation sources. This study also helps in choosing the optimum coupling parameters (in addition to other coupling safety factors).

Torque pulsation from the VFD harmonics is a natural excitation source in EMD-CS packages. Figure 28 shows a typical spectrum chart provided by motor vendors, showing magnitudes of dynamic torque pulsation at various VFD-output frequencies.

The motor's rated torque at the rated frequency is a critical parameter for this analysis. A 45-Hz-corner-frequency motor drive, which implies that the motor can produce the rated torque up to 45 Hz, and then switches to constant power between 45 Hz and 60 Hz. The pulsation magnitudes are referenced to the nominal motor torque.

A steady-state forced response torsional analysis is performed with this pulsation data to determine the maximum dynamic torque of each of the train equipment. A damping ratio of 1.67% (AF=30) is used based on the API and GMRC guidelines. However, lower damping ratios are also considered if the results show marginal safety factors.

Figure 29 shows the dynamic torque vs motor speed for all the torsional interferences identified in the earlier section - 1X, 2X, 3X and 24X (12f) – at the motor location. Figure 30 shows the same at the compressor location. Peak dynamic torque amplitudes derived from the forced response analysis are then used to calculate the alternating stress. The rated torque is used to calculate the mean stress. With those two parameters, an endurance study (Goodman diagram) is constructed [10] to confirm that the components shall have infinite life and sufficient safety factors from a High-cycle Fatigue perspective. For the motor and compressor locations, the Factors of Safety to the limit line are 12.4 and 11.1 respectively. This is repeated for each of the train equipment. Based on these results, the train is considered safe from torsional interference standpoint.
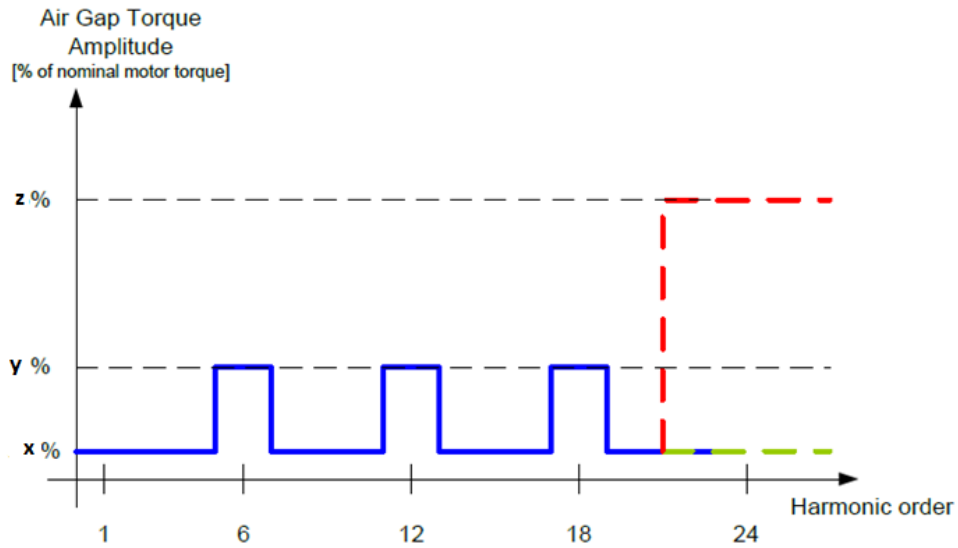

Figure 28 Motor air-gap torque harmonic envelope (pulsation torque)

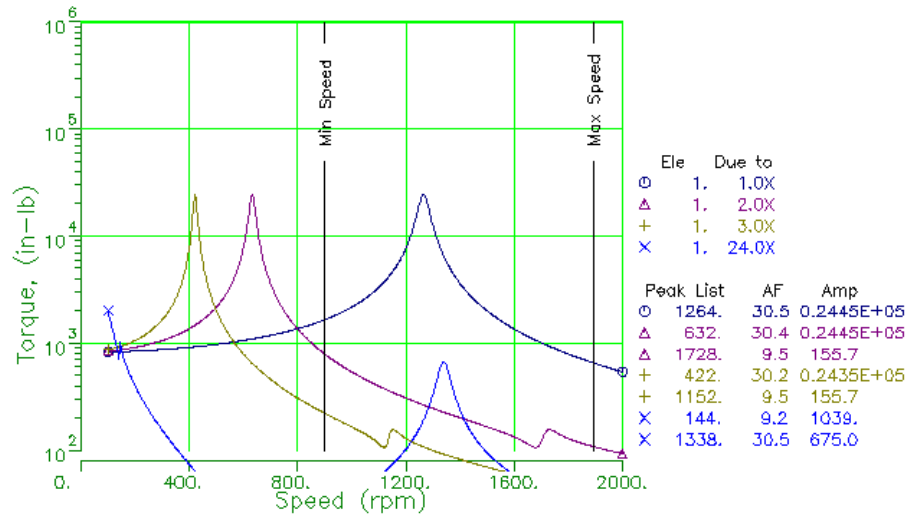EMD-STD; Motor1-8.7kHP-10StgC,Forced Resp-VFD pulsation
EMD

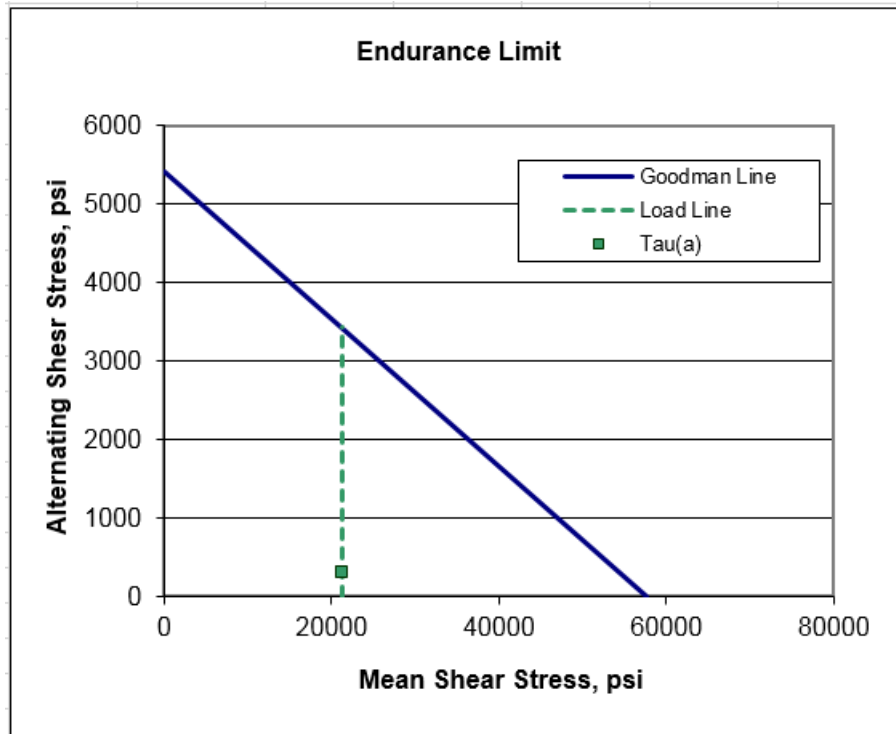**Figure 29 Results of forced response torsional analysis - at the motor location**

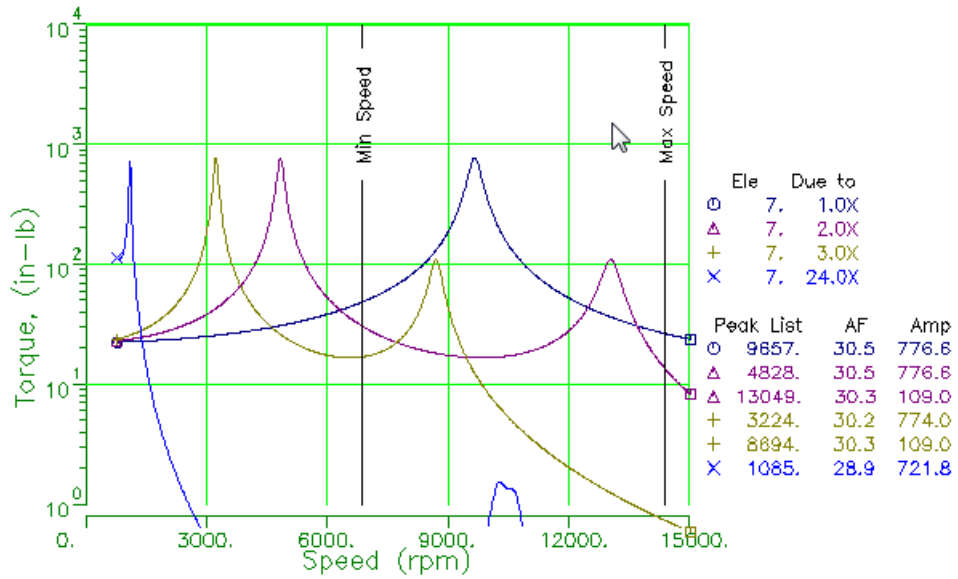**Figure 30 Endurance Limit from torque pulsation – Motor location – SF = 12.4**

Figure 31 Results of forced response analysis – at the compressor shaft location
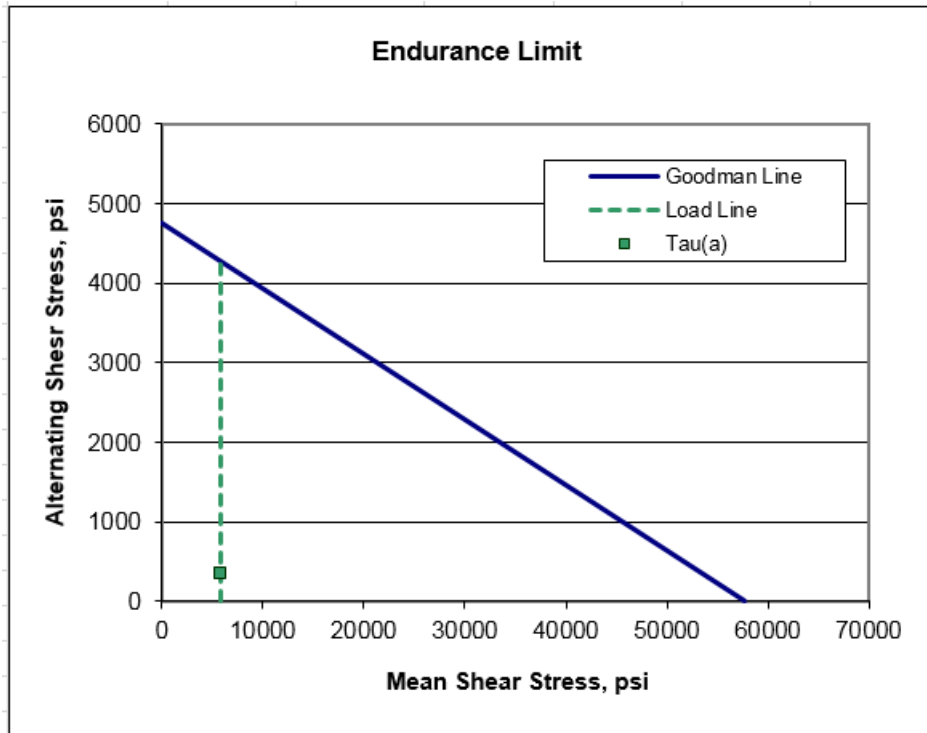

Figure 32 Endurance Limit from torque pulsation – Compressor location – SF = 11.1

FAULT TRANSIENT ANALYSIS

Electric-motor drives are subject to unexpected fault transients – such as phase-to-phase faults or phase-to-ground faults. They could either be 2-phase short circuits or 3-phase short circuits. The API guidelines require motor vendors and driven-equipment suppliers to consider these fault transients and ensure that the peak torques (expressed in terms of the PU – Per Unit rated torque) experienced by the train equipment do not exceed the component design limits.

Short-circuit information is provided by motor vendors. In the event of a short-circuit, the motor shaft experiences an instantaneous peak torque as the energy stored in the stator coils dissipate through the air-gap, then decays over a small amount of time. The air-gap torques at fault conditions are shown in Figures 32 and 33.
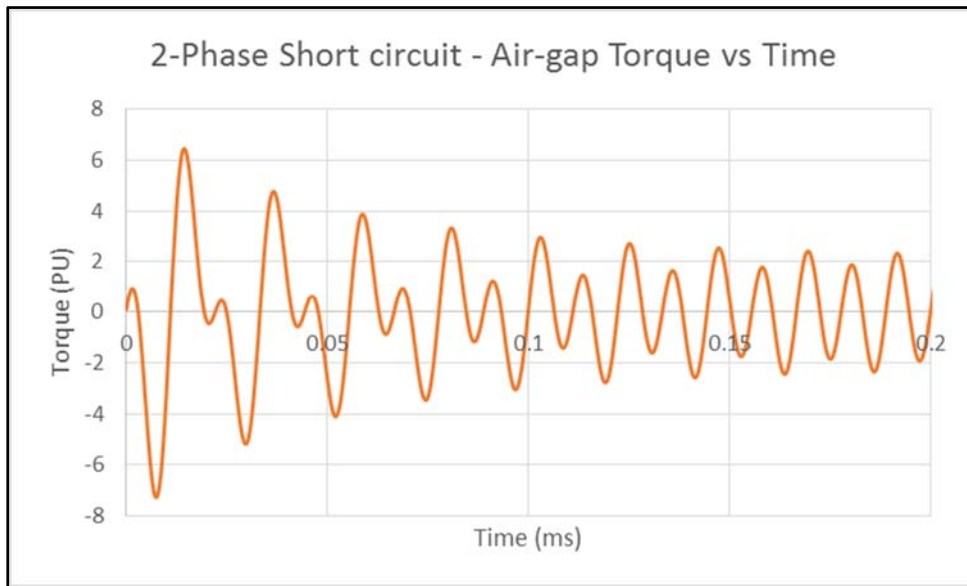

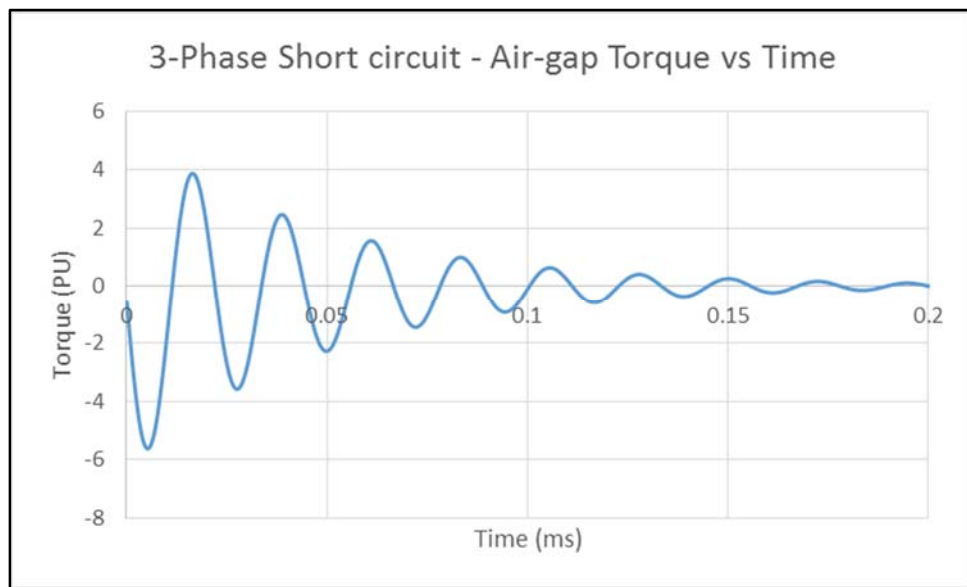**Figure 32 Fault transients - 2-Phase short circuit – Max PU = -7.3**

Figure 33 Fault transients - 2-Phase short circuit – Max PU = -5.6

A transient torsional analysis is performed using the above fault transients as input to the equations of motion shown earlier. Time-marching is achieved using Runge-Kutta method. The goal is to determine the propagation effect of the transient torque from the motor to other train equipment, their attenuation through the gearbox and the ability of the low-speed and high-speed couplings to handle the instantaneous torques. Figure 34 shows the results of transient torsional analysis from 2-phase short circuit fault event - peak torques at Motor shaft, Low-speed coupling, High-speed coupling and compressor shaft. Figure 35 shows the same for a 3-phase short circuit fault event.
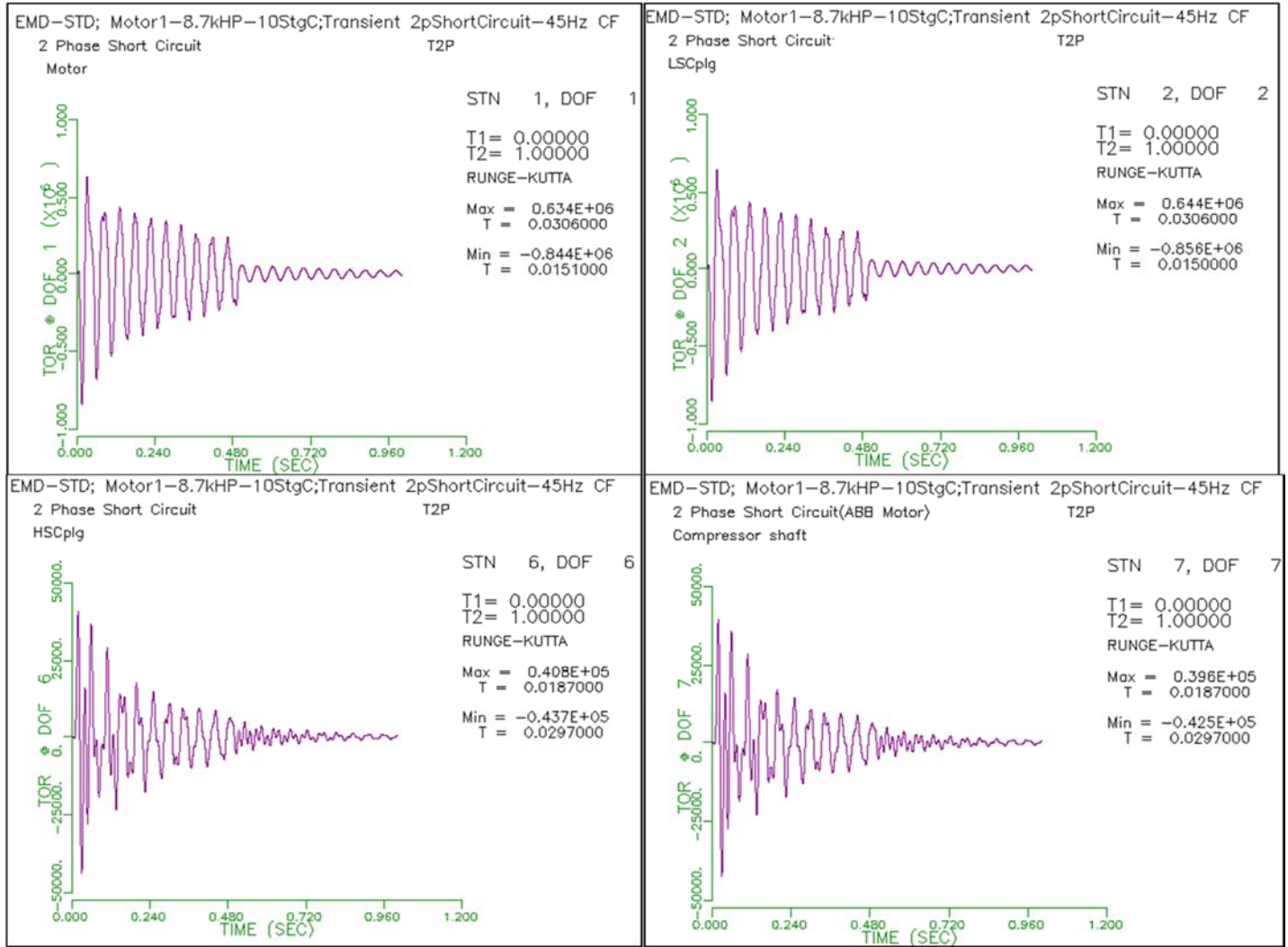

Figure 34 Results of transient torsional analysis from 2-phase short circuit fault event
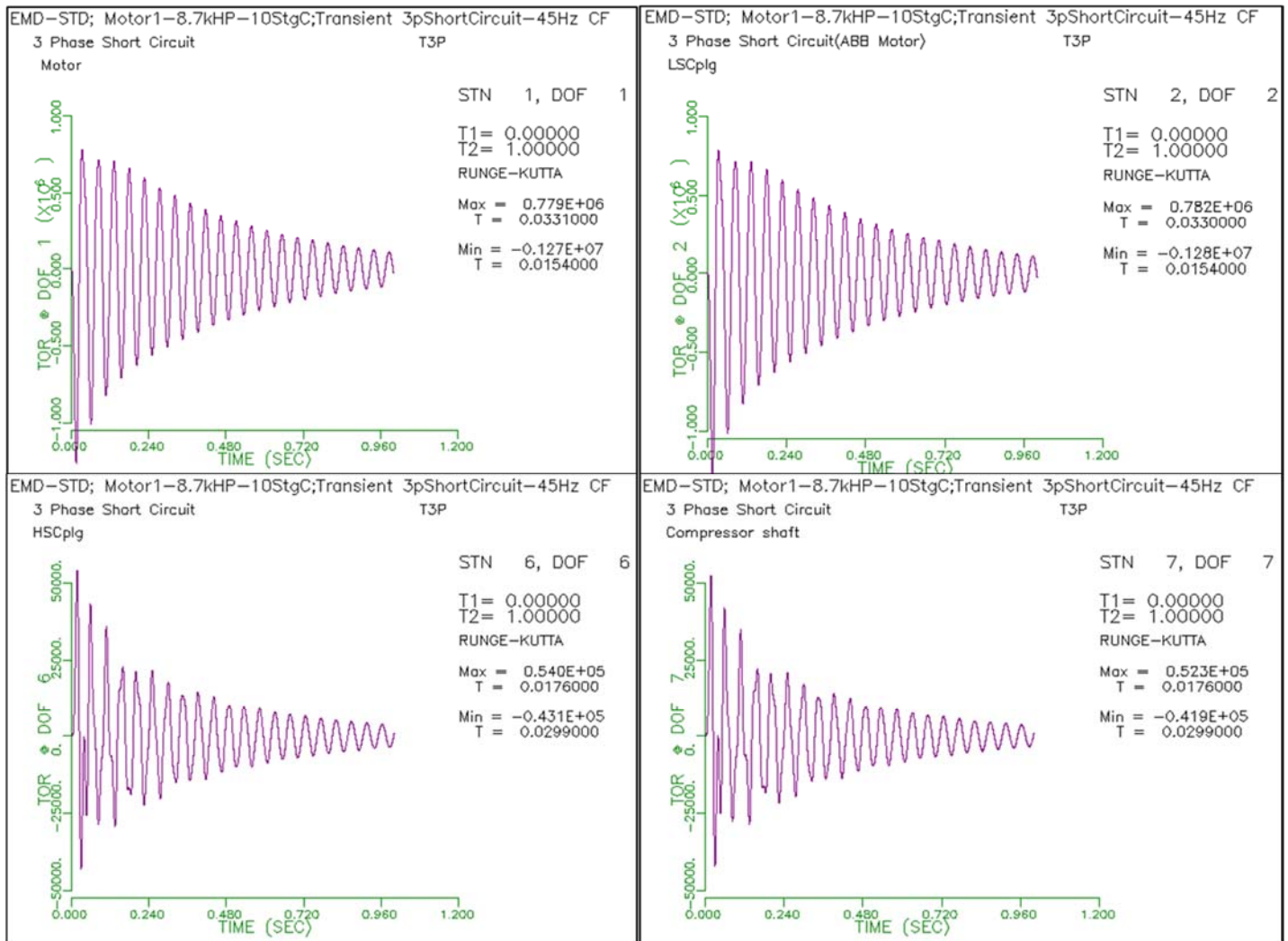
Figure 35 Results of transient torsional analysis from 3-phase short circuit fault event

Based on the peak torques transmitted during the fault events, the maximum shear stress occurring in the components are calculated. These are compared with the shear yield stress of the material to determine the safety factors. Also, the coupling designs are verified to be capable of transmitting the maximum momentary torque shown by this analysis. Short-circuit events may be one-time unexpected events, however, it is imperative to design the train equipment to survive such events for safety purposes.

CONCLUSIONS

To address the two topics of concern:

- starting of electric motors
- torsional integrity of the drive train,

This document provides a survey about possible starting methods of high-power motors that are operated directly at the grid. In the electric supply system, high starting currents cause partly high voltage dips thus endangering their stability. The grid conditions varying from strong to very weak grids or isolated networks, define whether a direct motor start is possible at all at the grid or whether alternative starting methods need to be specified. The grid connected load and thus the short-circuit capability are normally given and can only be influenced by larger, grid-structural measures. Therefore, alternative starting methods are the key approach with which the starting current and thus the voltage dip can be reduced during start-up. In addition, the duration of the voltage dip is reduced by the reduction of the counter torque and the mass moments of inertia which in this case was achieved by a variable speed hydrodynamic planetary gear (VSHD) drive system.

To deepen the discussion on torsional integrity, a methodology to ensure torsional integrity of VFD-EMD driving Gas Compressors is shown. The train's ability to handle torsional interference, torque pulsation from VFDs and short-circuit fault events without impacting the durability of the equipment is critical to end-users. To this end, analytical torsional models are developed with API and GMRC guidelines, and used to standardize train equipment. Results are shown for a 45-Hz corner frequency, 4-pole 8700 HP motor driving a 10-stage compressor. Interference diagrams and forced excitation response analysis show that the train is safe from a torsional standpoint. Transient analysis shows the peak torques can be handled by all the equipment

REFERENCES

[1] Kurz,R, White,R.C., Brun,K., 2012, "Upstream and Midstream Compression Applications- Part 2: Implications on Operation and Control of the Compression Equipment", ASME Paper GT2012-68006.

[2] PowerFactory version 15.2 User's Guide

[3] Kundur,P., 1994, Power System Stability and Control; EPRI; ISBN 0-07-0359858-X

[4] Fuenfer,R., 2009 "Where Compact & Simple Solutions Count – Variable Speed Planetary Gears", Offshore Mediterranean Conference, Ravenna, Doc-ID OMC-2009-049

[5] IEEE 1110-1991; Guide for Synchronous Generator Modeling Practices in Stability Analyses.

[6] Brun,K., Thorp,J., Meyenberg,C., Kurz,R. 2015, "Hydrodynamic Torque Converters for Oil&Gas Compression and Pumping Applications: Basic Principles, Performance Characteristics and Applications", 2015, Turbomachinery & Pump Symposium Houston

[7] Corbo,M.A., and Malanowski, S.B., 1996, "Practical Design Against Torsional Vibrations", Proc. 25th Turbomachinery Symposium, pp. 189-223.

[8] API 684: Standard Paragraphs Rotordynamic Tutorial: Lateral Critical Speeds, Unbalance Response, Stability, Train Torsionals, and Rotor Balancing

[9] "Application Guideline for Electric Motor Drive Equipment for Natural Gas Compressors", Version 4.0, May 2009, Gas Machinery Research Council and Southwest Research Institute.

[10] Shigley, J. E., and Mischke, C. R., Mechanical Engineering Design, New York: Mc-Graw Hill, Inc. 1989